The beginning of particle physics in the 50's with cosmic rays

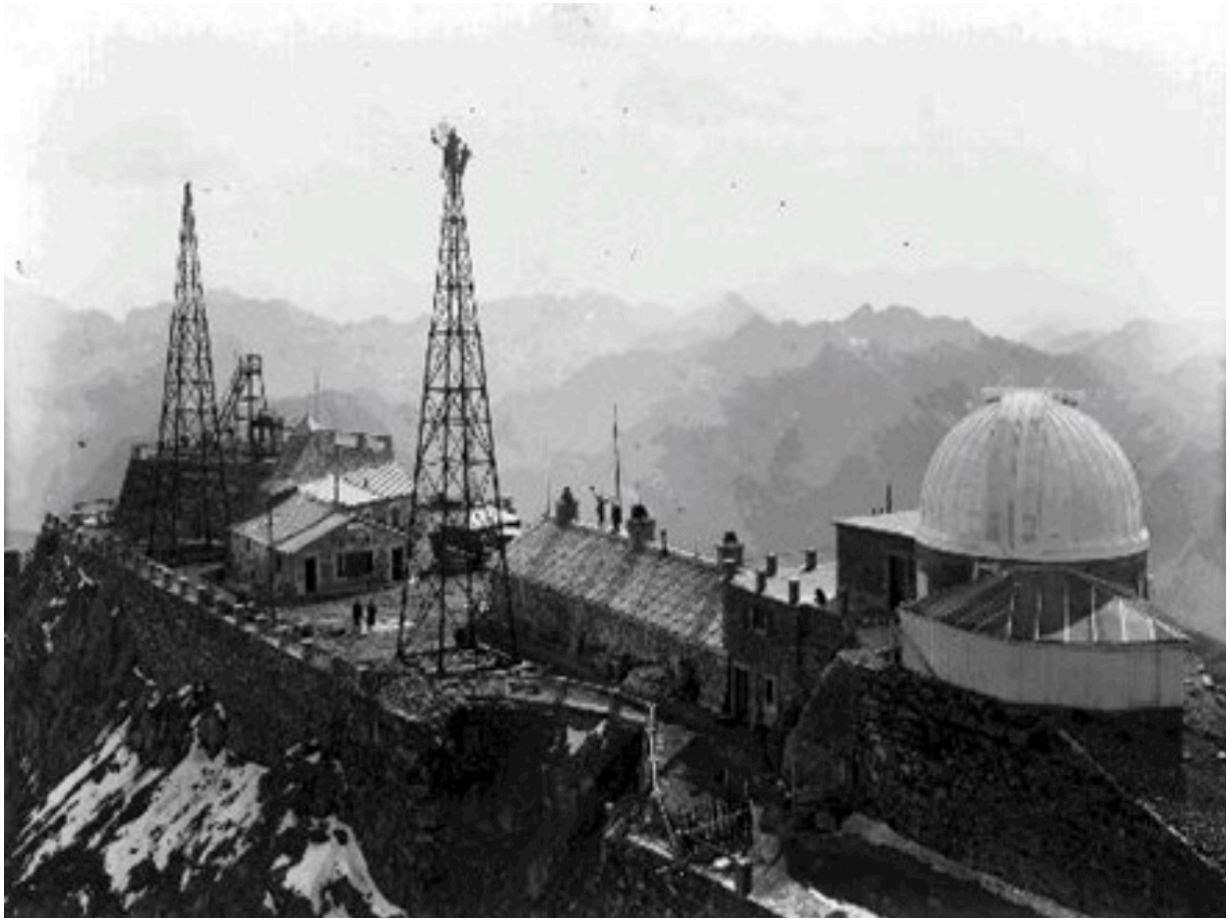

Cosmic Rays - I

Distinction between "primary" and "secondary" cosmic rays. Primaries are: protons, light Nuclei and γ. (+ others like electrons/positrons…)

Table 28.1: Relative abundances F of cosmic-ray nuclei at 10.6 GeV/nucleon normalized to oxygen (≡ 1) [7]. The oxygen flux at kinetic energy of 10.6 GeV/nucleon is 3.29×10^{-2} (m^2 s sr GeV/nucleon)$^{-1}$. Abundances of hydrogen and helium are from Refs. [3,4]. Note that one can not use these values to extend the cosmic-ray flux to high energy because the power law indicies for each element may differ slightly.

Z	Element	F	Z	Element	F
1	H	540	13–14	Al-Si	0.19
2	He	26	15–16	P-S	0.03
3–5	Li-B	0.40	17–18	Cl-Ar	0.01
6–8	C-O	2.20	19–20	K-Ca	0.02
9–10	F-Ne	0.30	21–25	Sc-Mn	0.05
11–12	Na-Mg	0.22	26–28	Fe-Ni	0.12

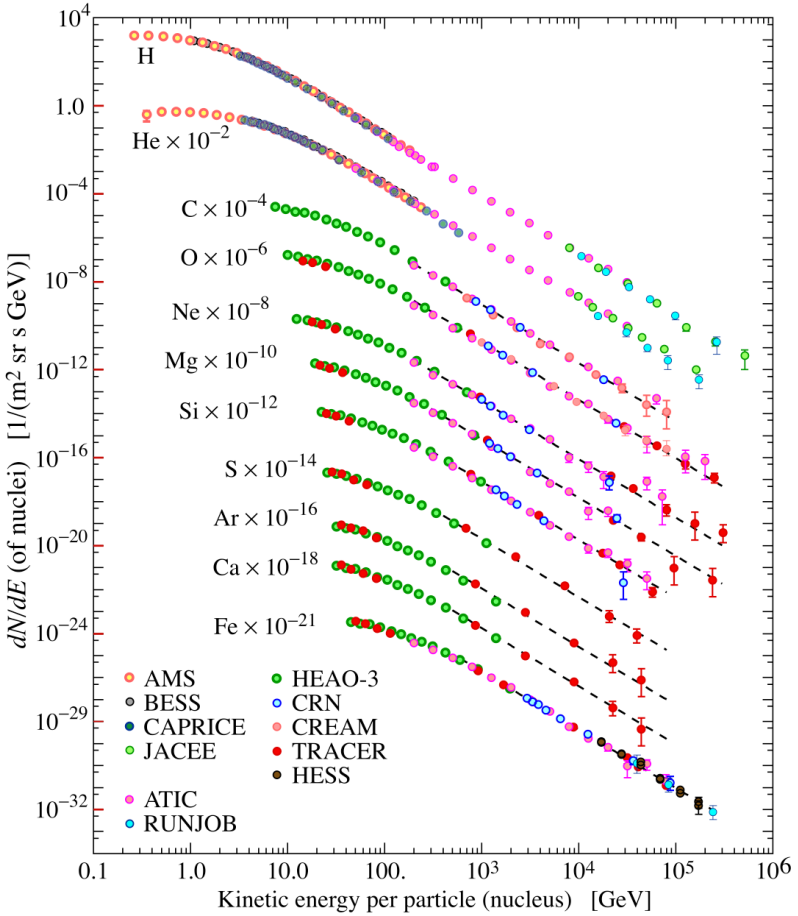

Figure 28.1: Fluxes of nuclei of the primary cosmic radiation in particles per energy-per-nucleus are plotted vs energy-per-nucleus using data from Refs. [2–13].

Cosmic rays - II

- At sea level cosmic rays are essentially muons. Rate ≈ 70 m^{-2} s^{-1} sr^{-1} ➔ 1 $cm^{-2}min^{-1}$ (≈ 2 Hz/dm^2) horiz. detector.
- Angular distribution: ≈ $\cos^2\theta$

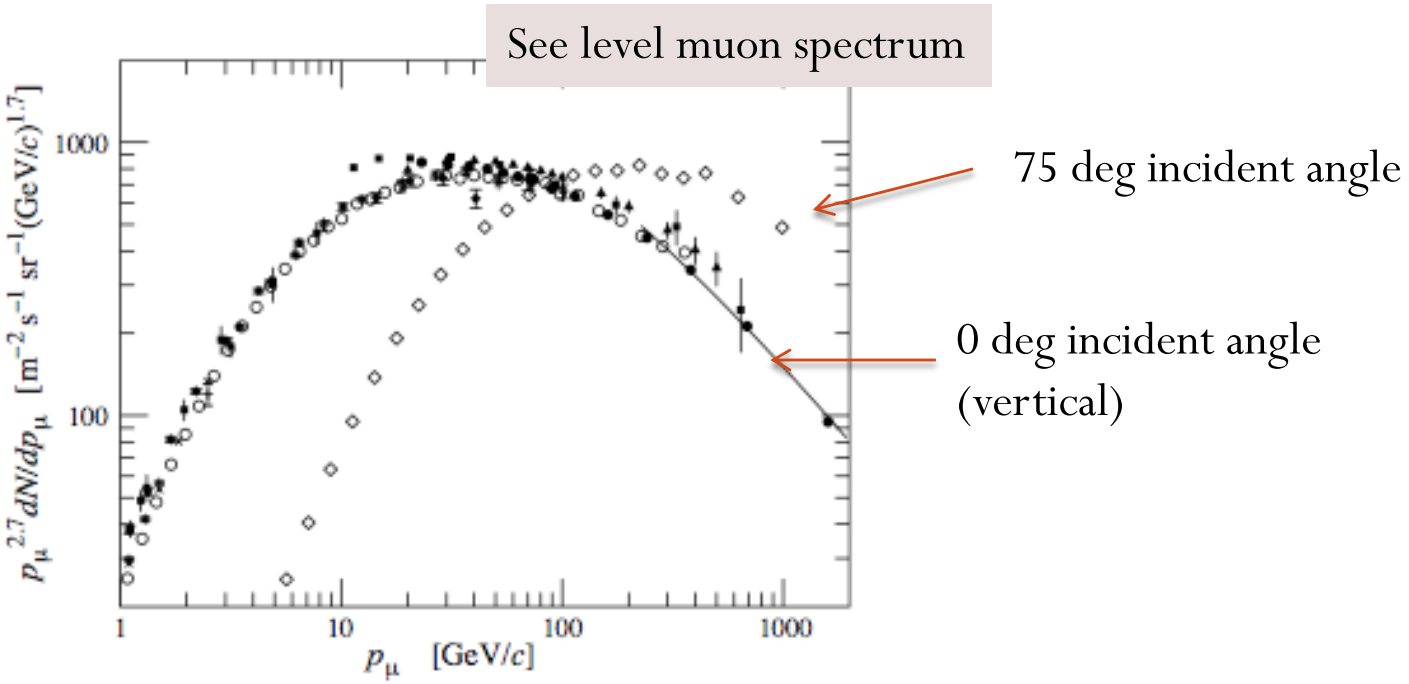

Cosmic rays - III

- Many discoveries of particles have been done in the past in experiments using cosmic rays as projectiles:
  - Positron
  - Muon
  - Pion
  - Kaon
- Today, large experiments use cosmic rays for specific studies:
  - Astrophysical objects (AGN, pulsars, anisotropies,…)
  - Fundamental phsyics phenomena (ZKP effect) profiting of the ultra high energy of the primary
  - Matter/Antimatter and Dark Matter
- Experiments located in the ground, underground (or deep in the oceans) and in the space

Present cosmic ray experiments

Underwater experiment: ANTARES

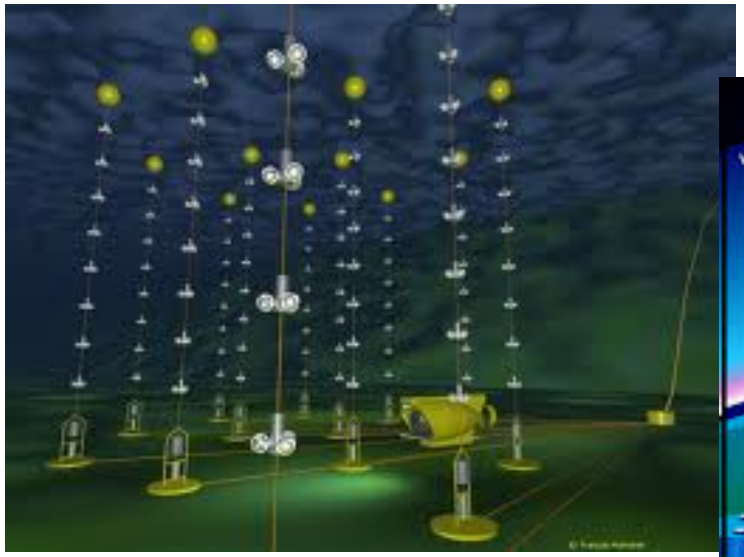

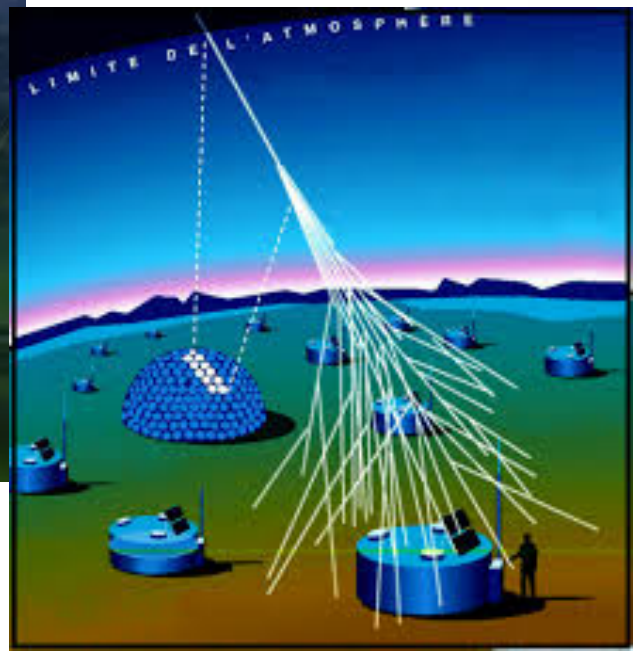

Ground based experiment: AUGER

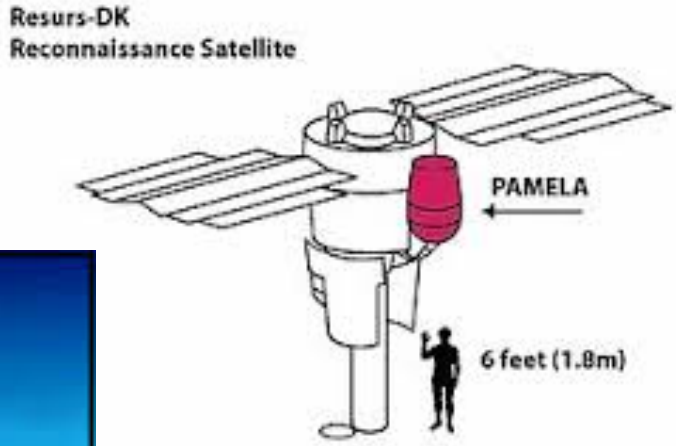

Satellite based experiment: PAMELA

We will discuss AMS in a specific lecture.

{

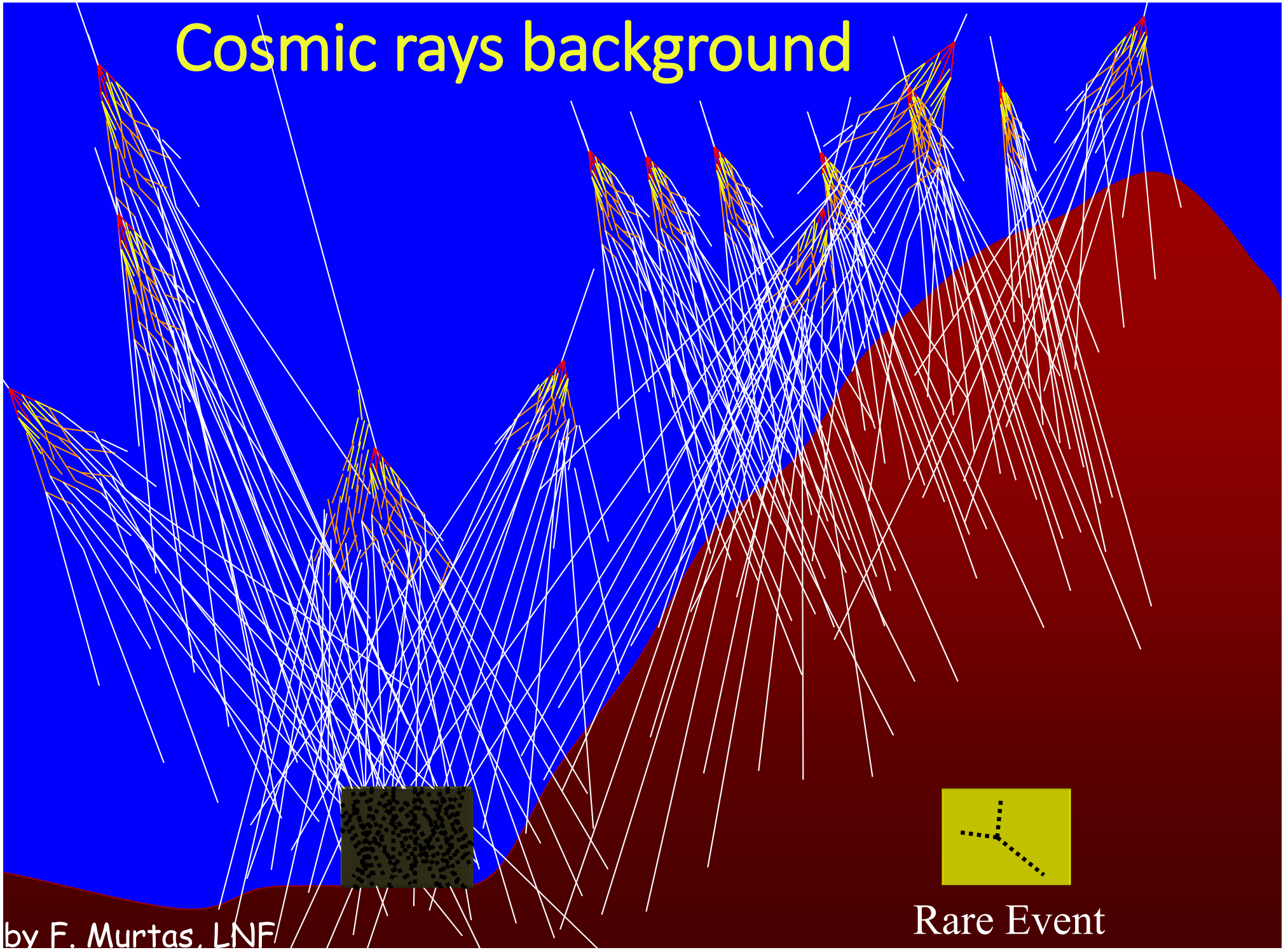
Cosmic rays background
Rare Event
by F. Murtas, LNF

Primary cosmic rays

~90% protons, 9% ^{4}He nuclei, and ~1% heavier particles, hit the earth atmosphere at a rate of about 1000 m^{-2}s^{-1}

(+ relativistic electrons, X-rays and γ rays and solar and SN neutrinos)

Secondary cosmic rays

The interaction of primary cosmic rays with atmospheric nuclei generates:

- π and k mesons
- muons
- electrons and positrons
- neutrons and secondary protons
- e.m. radiation
- atmospheric neutrinos

$$p + A \longrightarrow p + A + n\pi^{\pm} + m\pi^{0}$$

$$\pi^{+} \longrightarrow \mu^{+} + \nu_{\mu}$$

$$\pi^{0} \longrightarrow \gamma + \gamma$$

$$\mu^{+} \longrightarrow e^{+} + \nu_{e} + \bar{\nu}_{\mu}$$

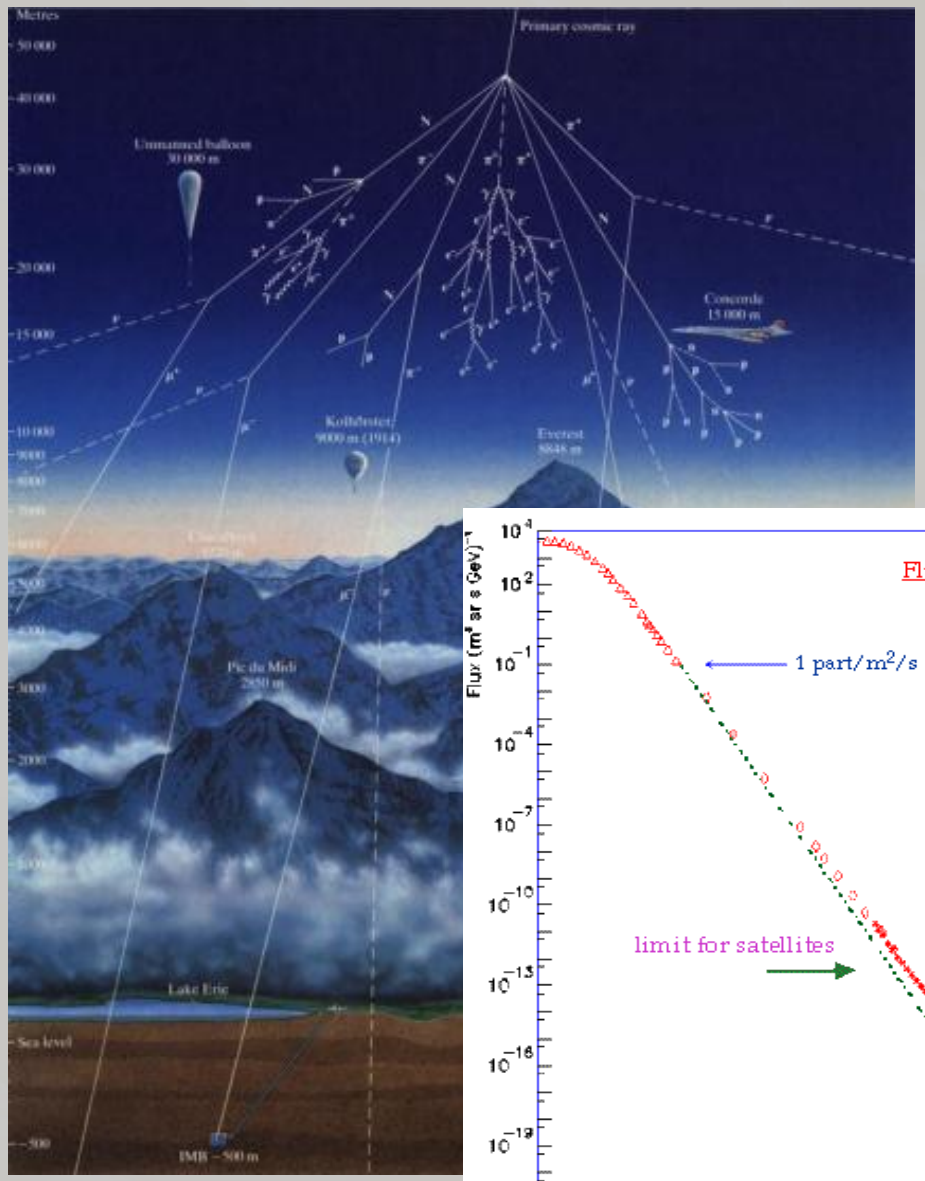

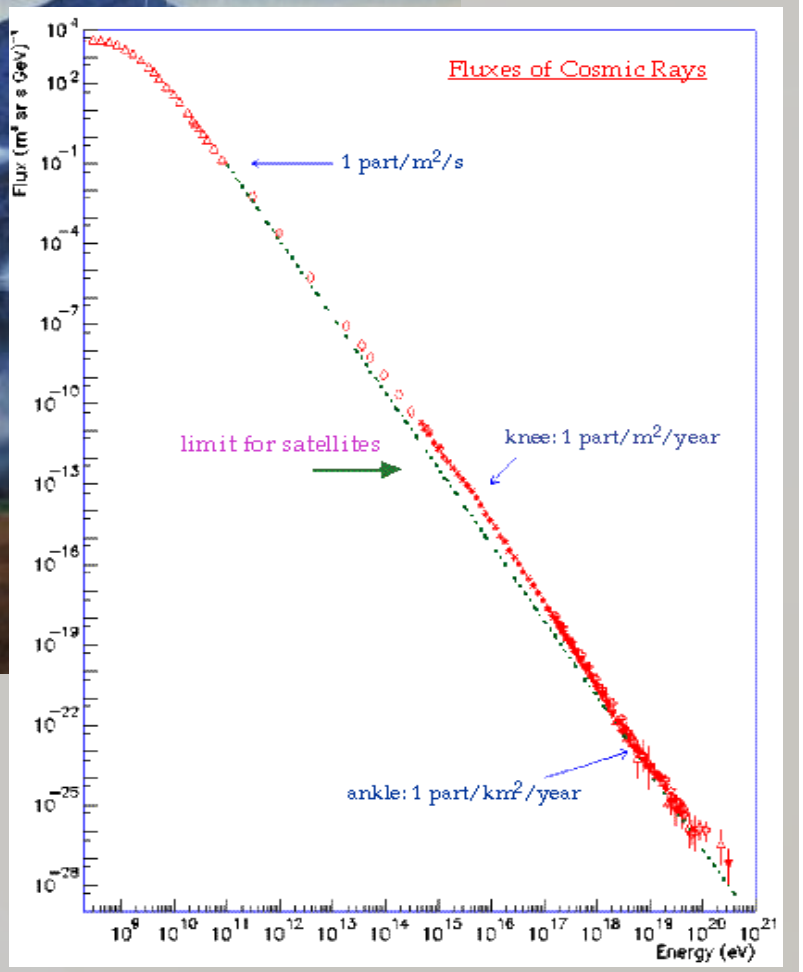

Example of cosmic rays reduction in a underground lab

- Muoni
  - 10^6
- Neutroni
  - 10^3
- Fotoni (gamma)
  - 10

LNGS

Depth: 1400 m

(**3800 m w.e.**)

Muon Flux

1.1 μ m^{-2} h^{-1}

Thanks to this cosmic silence, underground laboratories provide the low radioactive background environment necessary to host key experiments to search for extremely rare phenomena in the field of particle and astroparticle physics, nuclear astrophysics and other disciplines

Deep Underground Laboratories (>1000 mwe) in the world

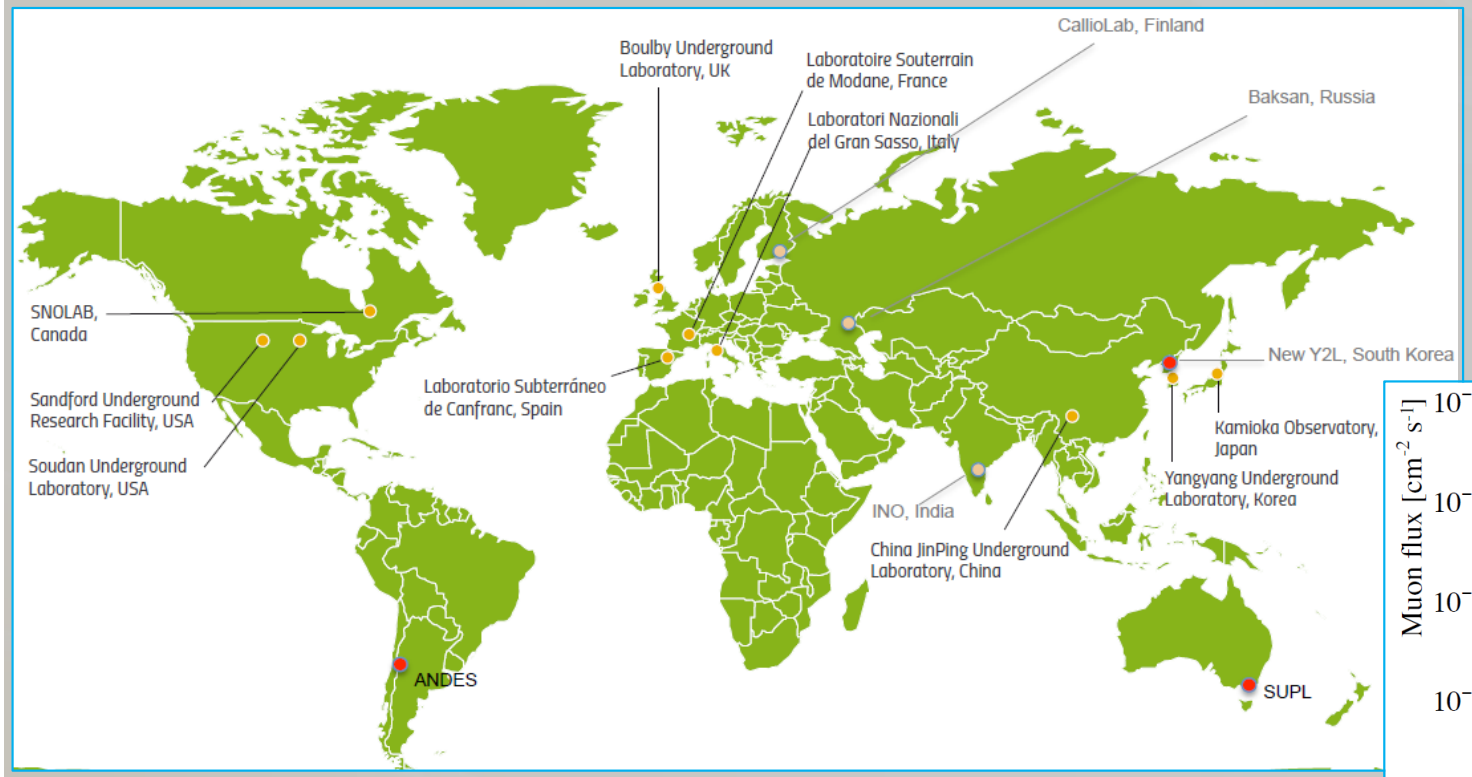

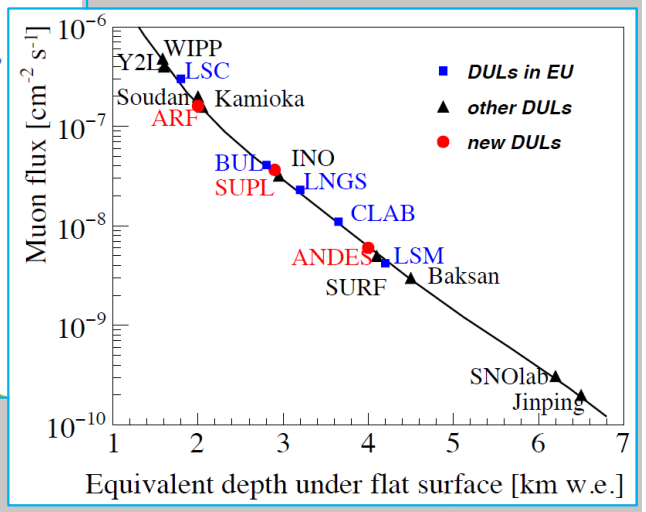

	SNOLab Canada	LNGS Italy	LSC Spain	BUL UK	LSM France	CallioLab Finland	Baksan Russia	SURF USA	CJPL China	Kamioka Japan	Y2L South Korea
since	2003	1987	2010	1989	1982	1995	1967	2007	2009	1983	2003
Volume (m^3)	30000	180000	10000	7200	3500	1000	23000	7160	300000 nearly completed	150000	5000
depth (m)	2070	1400	850	1100	1700	1440	1700	1500	2400	1000	700
access	V	H	H	V	H	V+drive in	H	V	H	H	drive in
Average Rn (Bq/m3)	130	80	100	<3	15	70	40	300	40	80	40

Underground Laboratories in the world

Europe

- Boulby: Boulby Palmer Laboratory (UK)
- LNGS: Laboratorio Nazionale del Gran Sasso (Italy)
- LSC: Laboratorio Subterráneo de Canfranc (Spain)
- LSM: Laboratoire Subterrain de Modane (France)
- CallioLab: Centre for Underground Physics in Pyhäsalmi (Finland)
- Solotvina Underground Laboratory (Ukraine)
- Baksan: Baksan Neutrino Observatory (Russia)

Asia

- Y2L: YangYang Laboratory (Korea)
- Oto Cosmo Observatory (Japan)
- Kamioka: Kamioka Observatory (Japan)
- INO: India based Neutrino Observatory (India)
- CJPL: China Jinping Underground Laboratory (China)

North America

- SNOLab: Sudbury Neutrino Observatory (Canada)
- SUL: Soudan Underground Laboratory (USA)
- SURF: Sanford Underground Research Facility (USA)

Gran Sasso Laboratory

The largest underground laboratory in the world

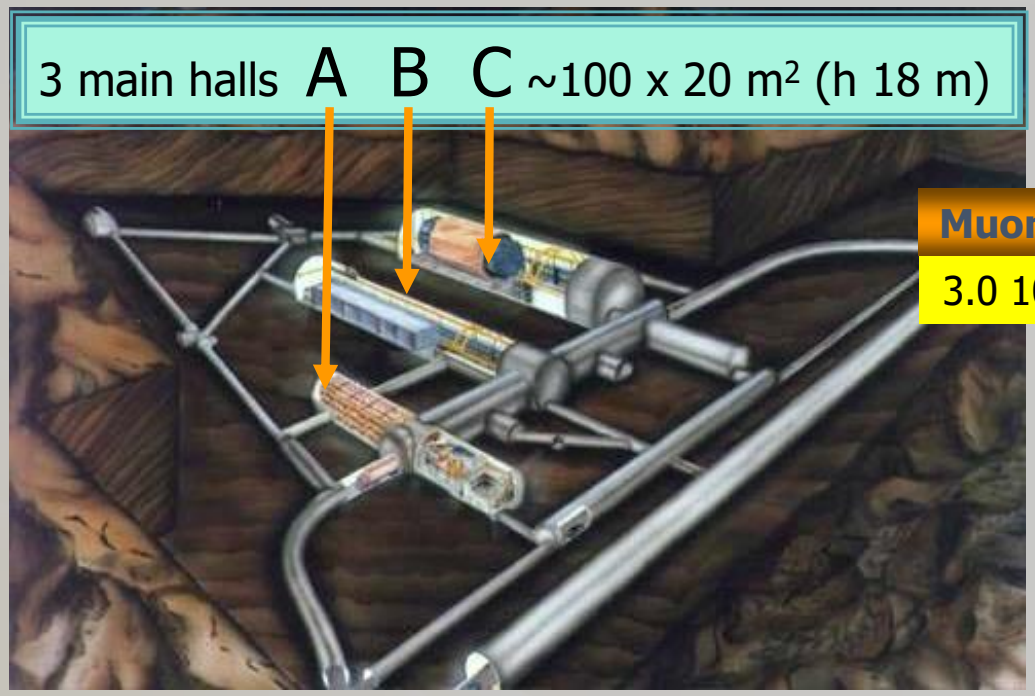

Currently 1100 scientists from 29 countries are taking part in the experimental activities

Muon Flux
3.0 10^{-4} μ m^{-2} s^{-1}

Neutron Flux	
2.92 10^{-6} n cm^{-2} s^{-1}	(0-1 keV)
0.86 10^{-6} n cm^{-2} s^{-1}	(> 1 keV)

Depth: 1400 m (**3800 m w.e.**)

3 halls surface ~ 6000 m^2

Total surface: 17300 m^2

Volume: **180000** m^3

Rn in air: 50-100 Bq/m^3

Air-ventilation: 1lab volume/3.5 h

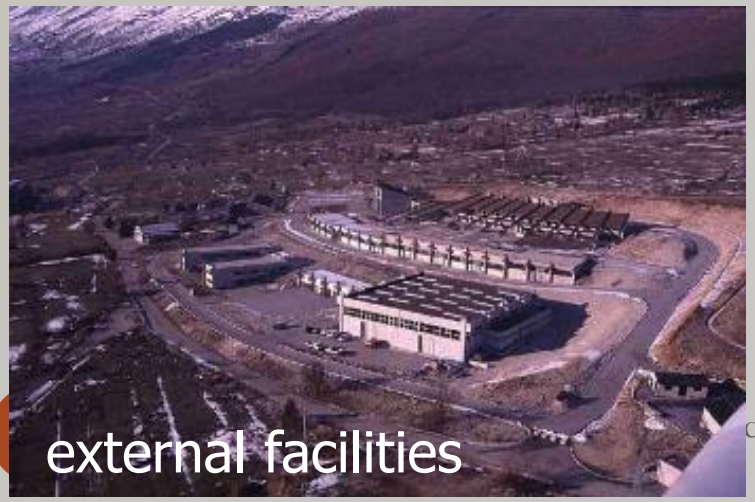

Primordial Radionuclides			
^{238}U	0.42 ppm	Rock	(Hall B)
	1.05 ppm	Concrete	All Halls
^{232}Th	0.062 ppm	Rock	(Hall B)
	0.656 ppm	Concrete	All Halls
K	160 ppm	Rock	

CS

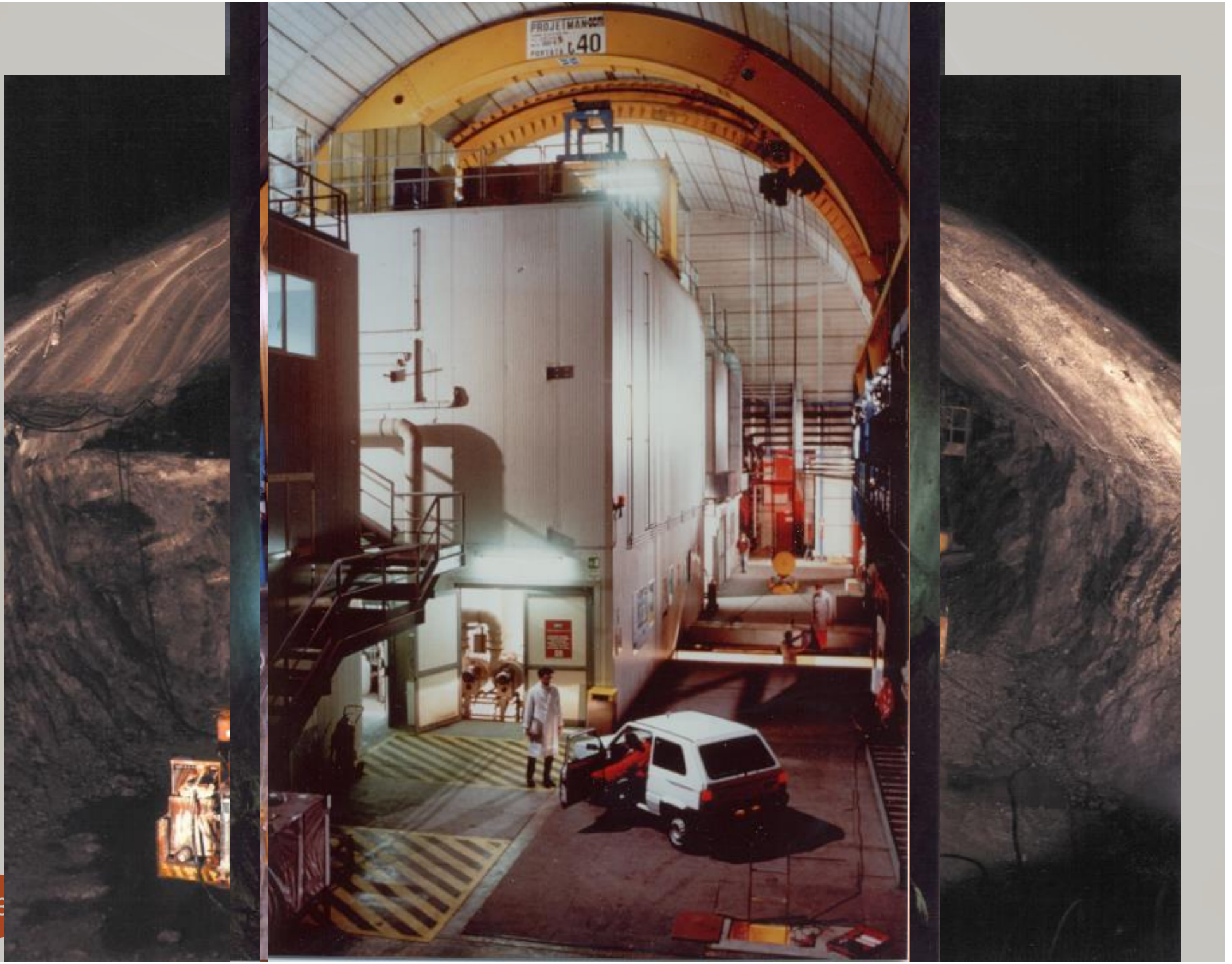
PROJET MAN-SCR
40

}

AMS

- Aim of the experiment:
  - measure e^+/e^- spectra, fluxes and ratios;
  - measure proton and ions spectra fluxes and ratios
  - look for possible dark matter signals
  - measure flux of primary anti-protons
- Detector requirements
  - measure the sign of the charge (e^+/e^- discrimination)
  - measure the Z of a ion
  - measure particle velocity

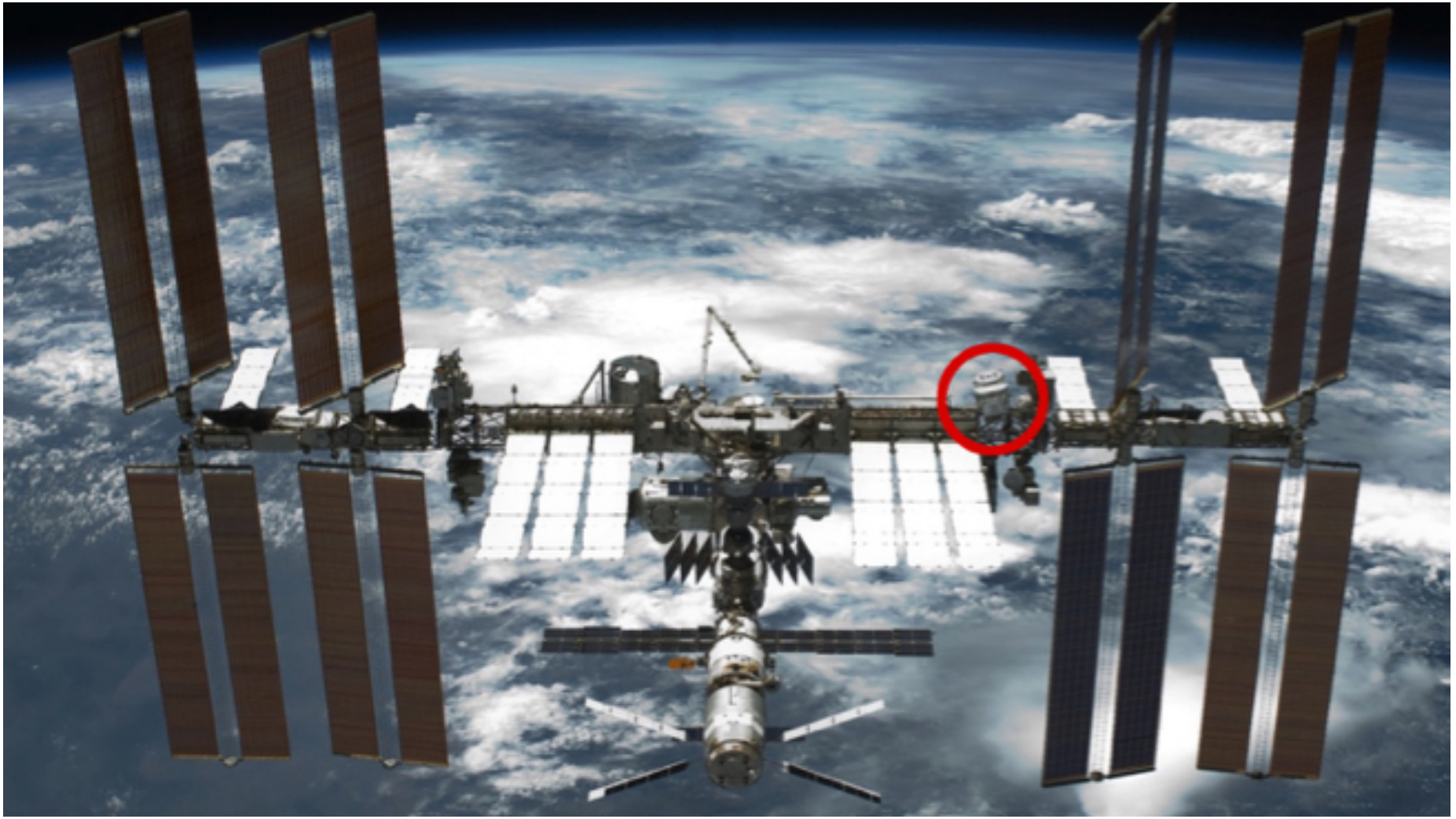

AMS: an experiment on the space station.

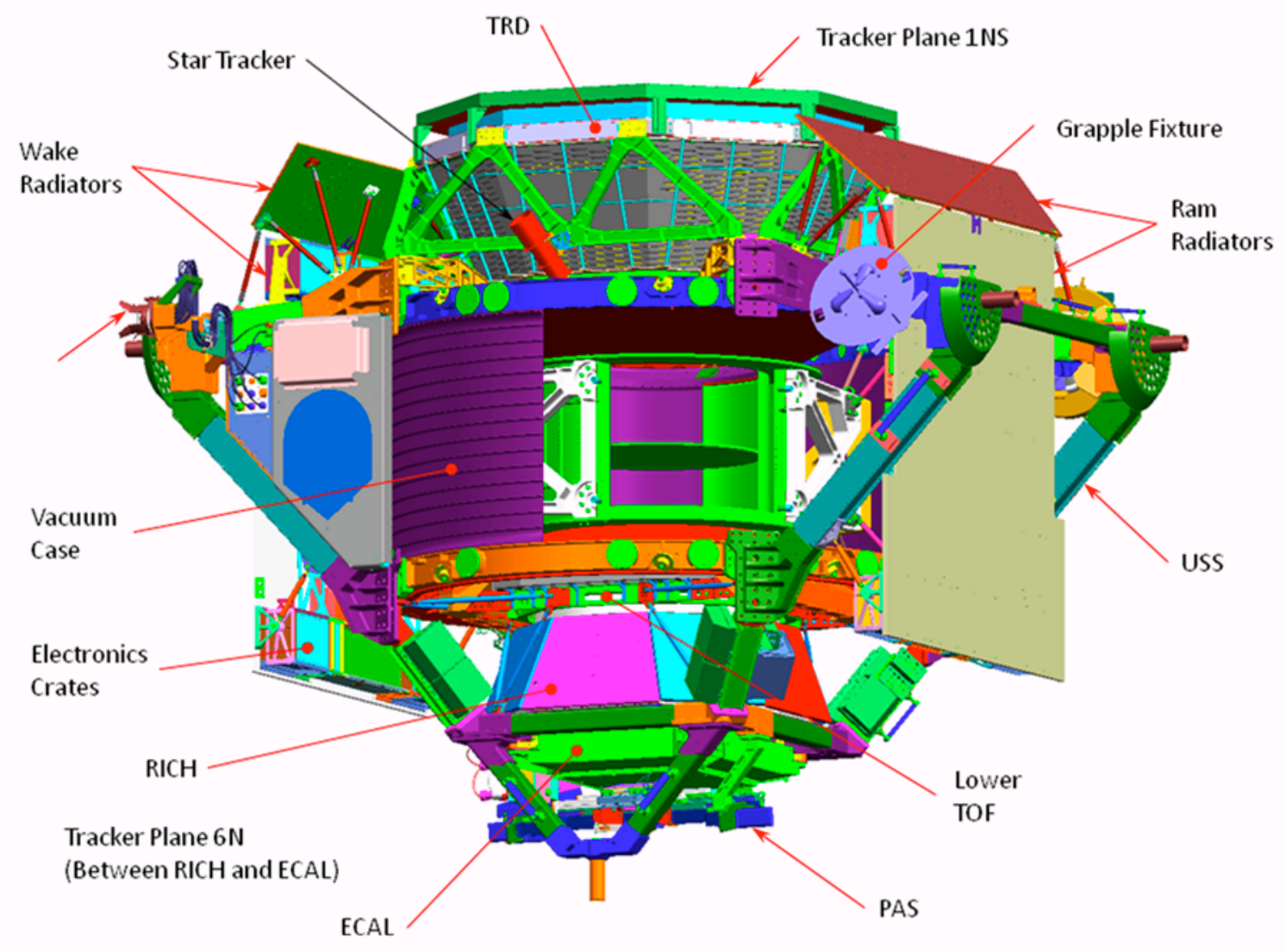

AMS – subdetectors.

≈ 4 m

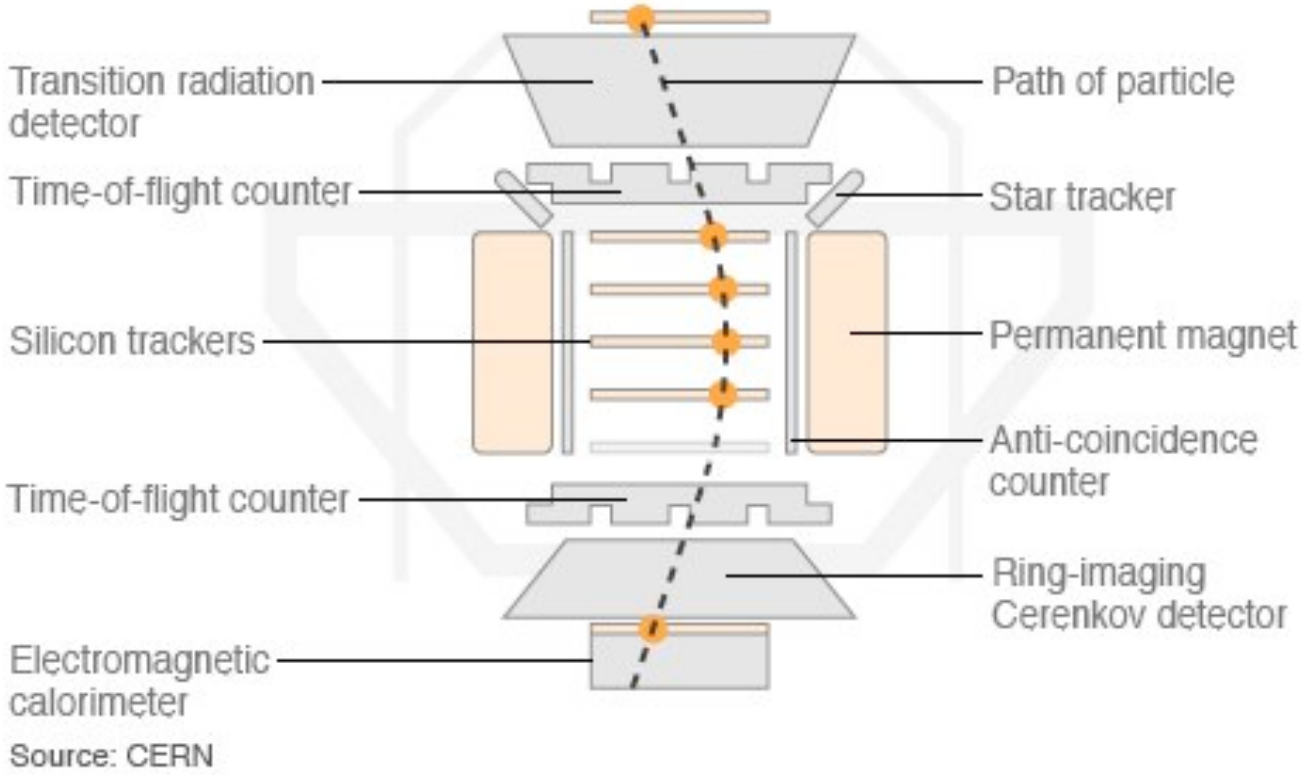

AMS-02
18 years on the ISS

TRD
Identify e+, e-

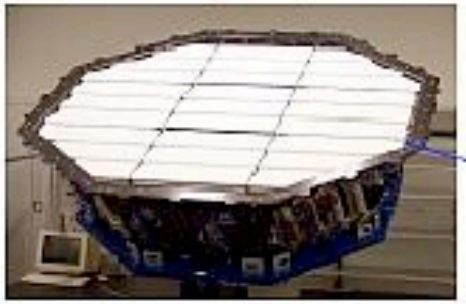

Silicon Tracker
Z, P

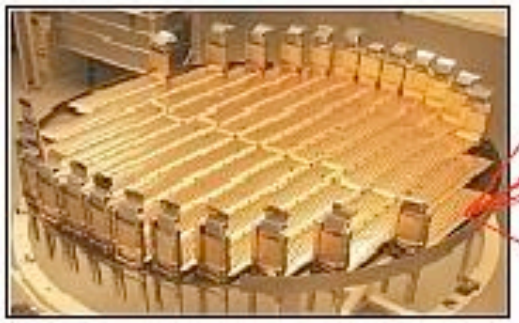

ECAL
E of e+, e-, γ

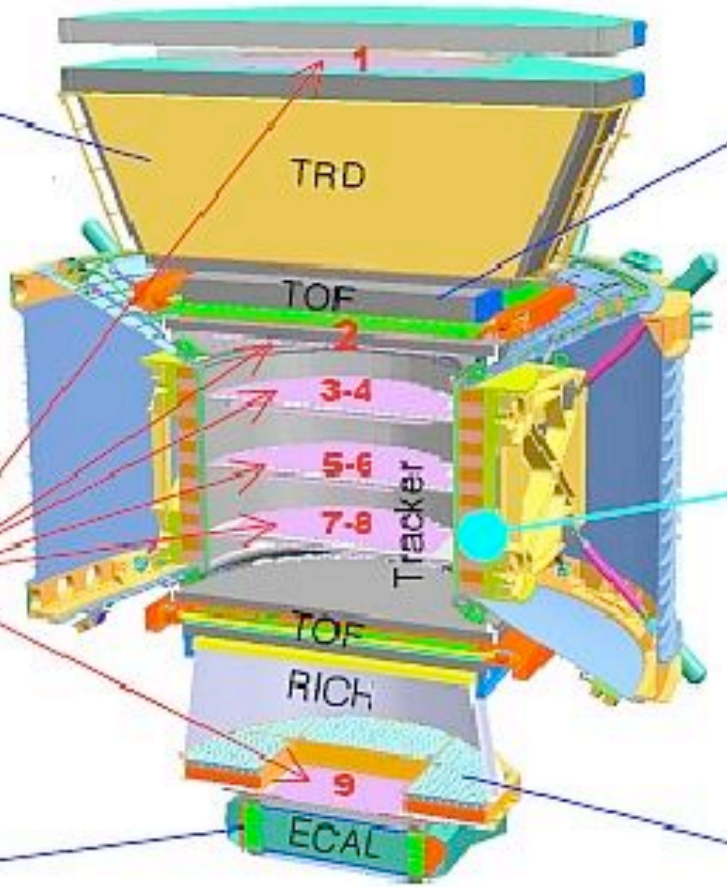

TOF
Z, E

Magnet
±Z

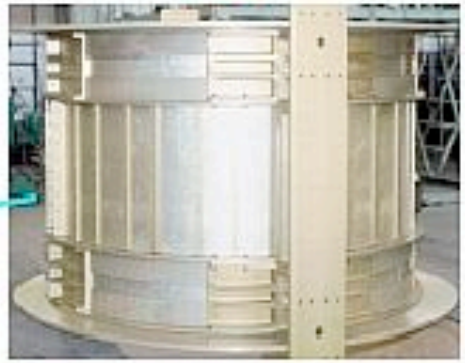

RICH
Z, E

AMS - Events

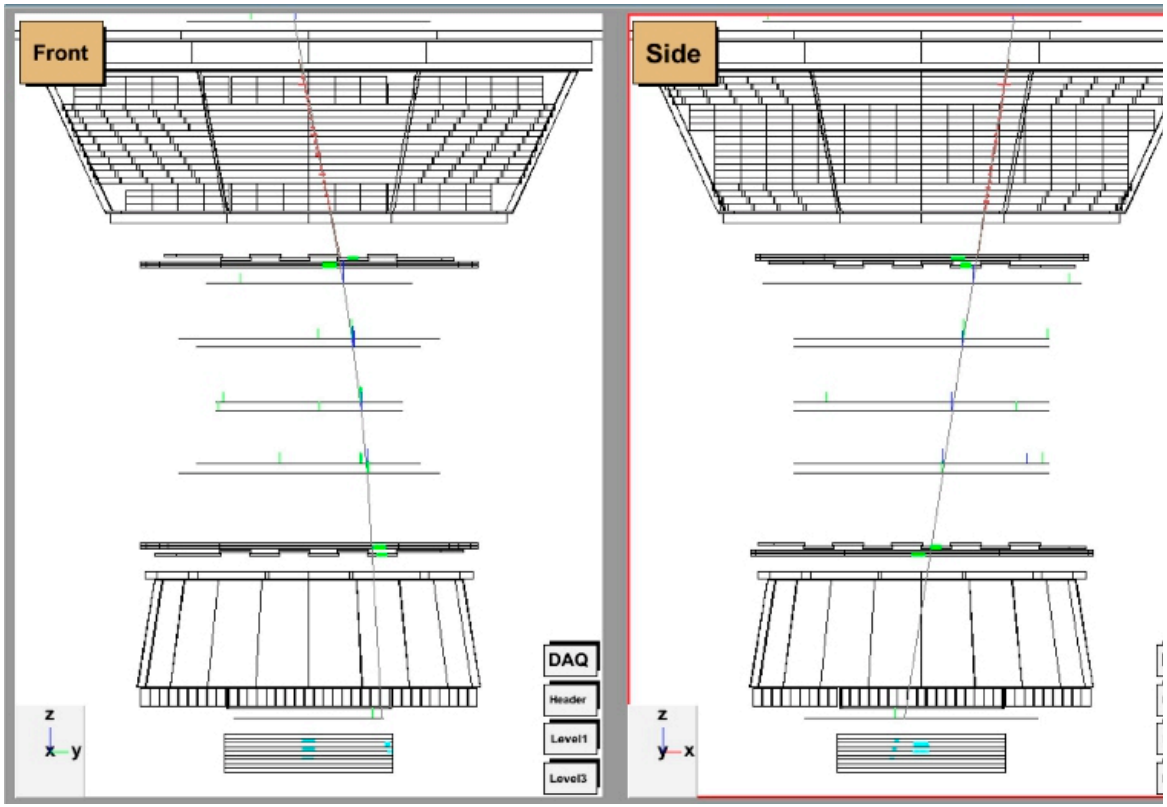

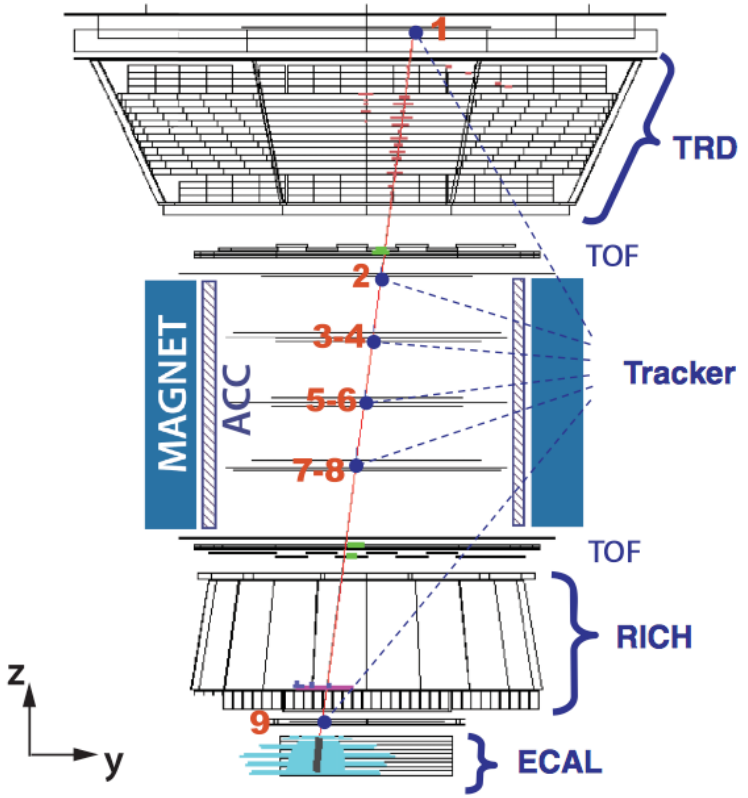

FIG. 1 (color). A 1.03 TeV electron event as measured by the AMS detector on the ISS in the bending (y-z) plane. Tracker planes 1–9 measure the particle charge and momentum. The TRD identifies the particle as an electron. The TOF measures the charge and ensures that the particle is downward-going. The RICH independently measures the charge and velocity. The ECAL measures the 3D shower profile, independently identifies the particle as an electron, and measures its energy. An electron is identified by (i) an electron signal in the TRD, (ii) an electron signal in the ECAL, and (iii) the matching of the ECAL shower energy and the momentum measured with the tracker and magnet.

AMS – subdetector functionalities

AMS: A TeV Magnetic Spectrometer in Space

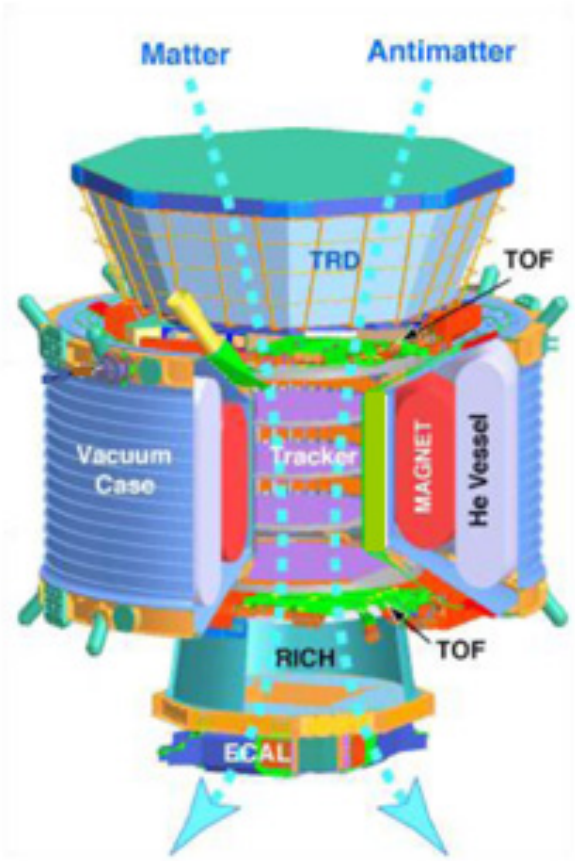

Data Signature of Various Particles in Each Detector

	e^-	P	Fe	e^+	$\bar{P}$	$\overline{He}$
TRD						
TOF						
Tracker + Magnet						
RICH						
ECAL						
Physics example	Cosmic Ray Physics Strangelets			Dark matter		Antimatter

AMS – discrimination - I

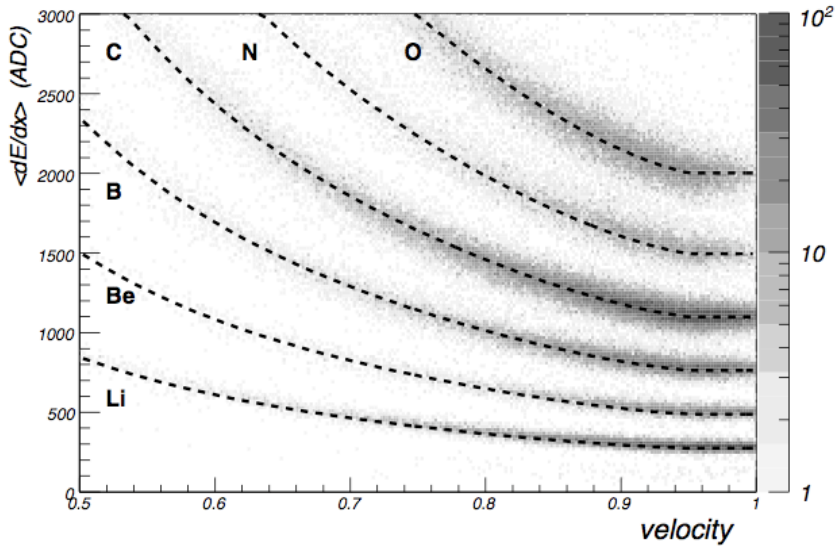

Fig. 2: Signal amplitude (ADC) of the mean energy loss in the silicon tracker vs velocity. Nuclear families fall into distinct charge bands. MPVs of the $P_Z^k(x_k, \beta)$ functions are superimposed for Z=3 to 8 (dashed lines).

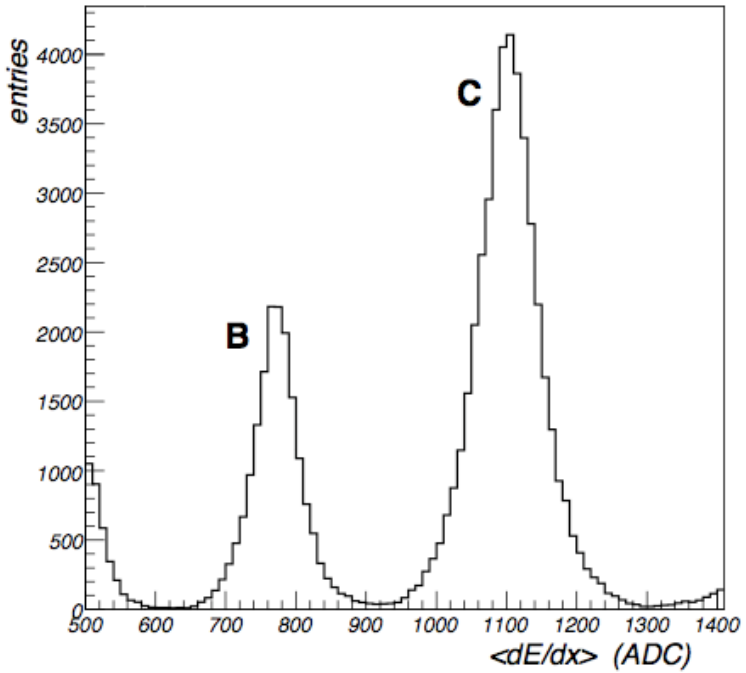

Fig. 3: Charge histograms in the B and C region. The signal amplitudes of Fig 2 are here equalized to $\beta \equiv 1$. Boron and Carbon families fall in distinct charge peaks.

AMS – discrimination - II

TRD estimator:
LogL(electron)/LogL(proton)

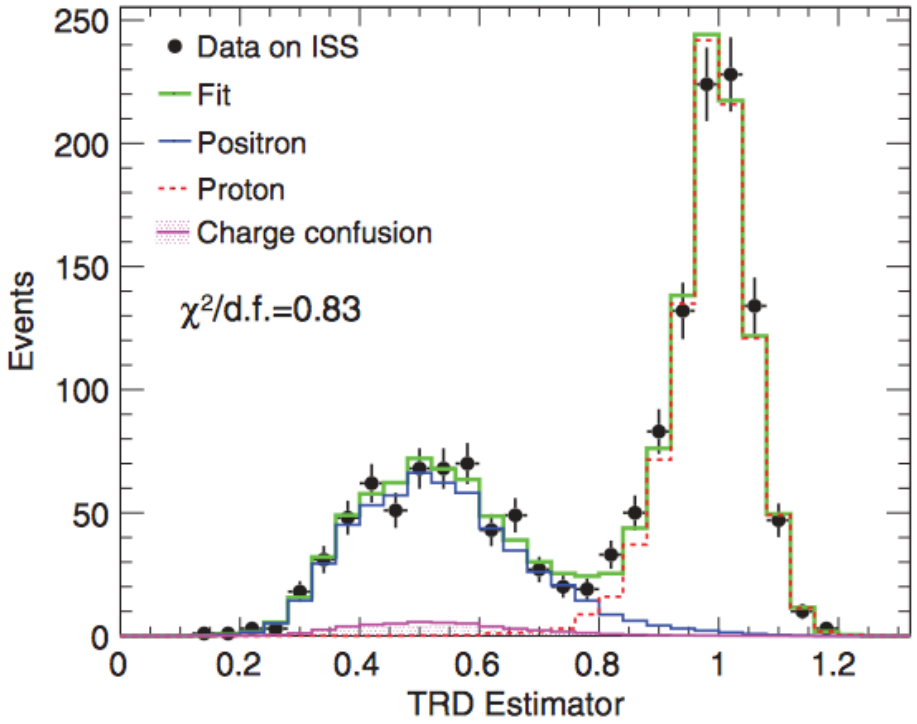

FIG. 3 (color). Separation power of the TRD estimator in the energy range 83.2–100 GeV for the positively charged selected data sample. For each energy bin, the positron and proton reference spectra are fitted to the data to obtain the numbers of positrons and protons.

AMS – most important results

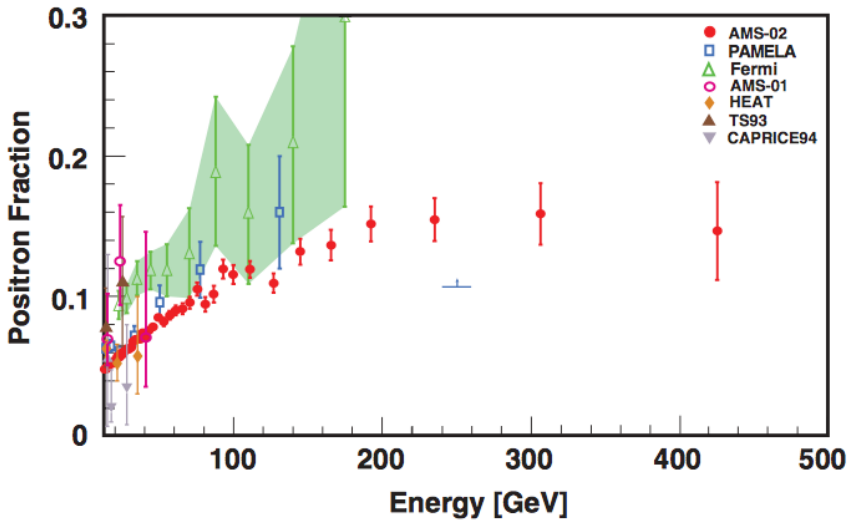

FIG. 3 (color). The positron fraction above 10 GeV, where it begins to increase. The present measurement extends the energy range to 500 GeV and demonstrates that, above ~200 GeV, the positron fraction is no longer increasing. Measurements from PAMELA [21] (the horizontal blue line is their lower limit), Fermi-LAT [22], and other experiments [17–20] are also shown.

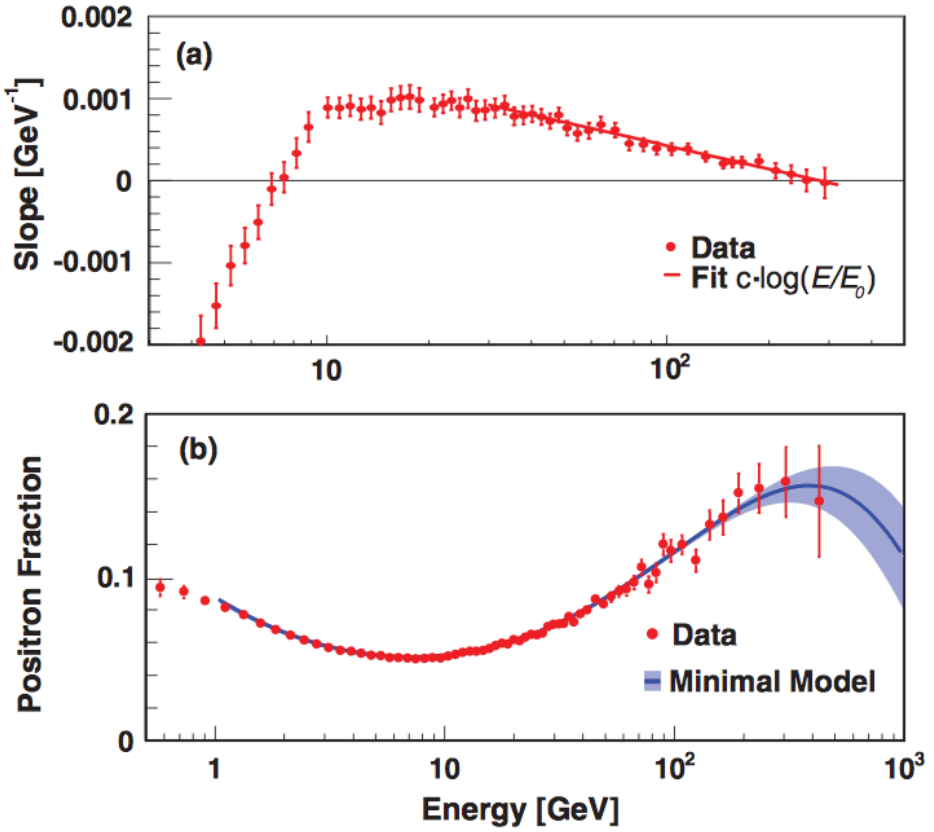

FIG. 4 (color). (a) The slope of the positron fraction vs energy over the entire energy range (the values of the slope below 4 GeV are off scale). The line is a logarithmic fit to the data above 30 GeV. (b) The positron fraction measured by AMS and the fit of a minimal model (solid curve, see text) and the 68% C.L. range of the fit parameters (shaded). For this fit, both the data and the model are integrated over the bin width. The error bars are the quadratic sum of the statistical and systematic uncertainties. Horizontally, the points are placed at the center of each bin.

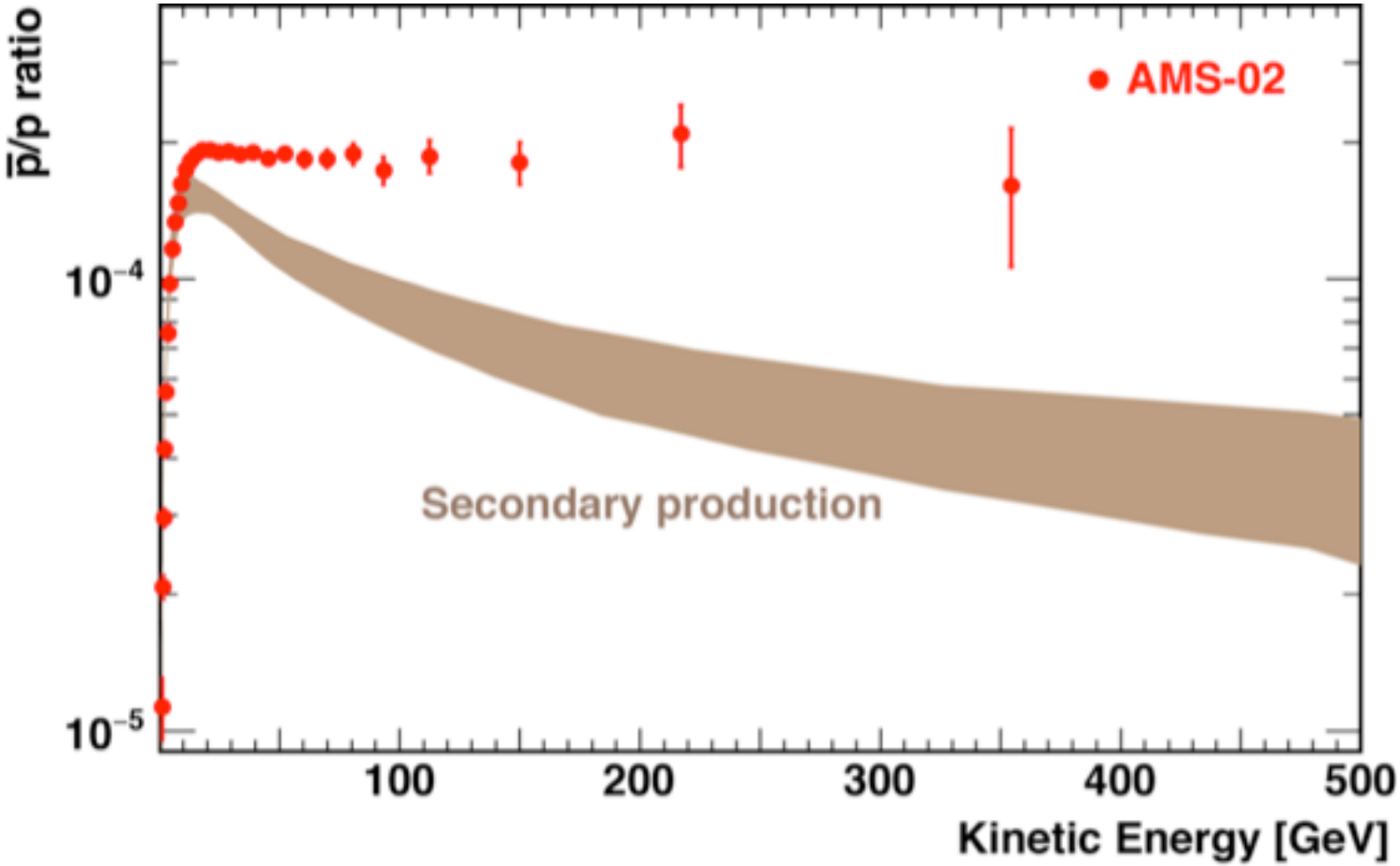
$\bar{p}/p$ ratio
AMS-02
Secondary production
10^{-4}
10^{-5}
100
200
300
400
500
Kinetic Energy [GeV]

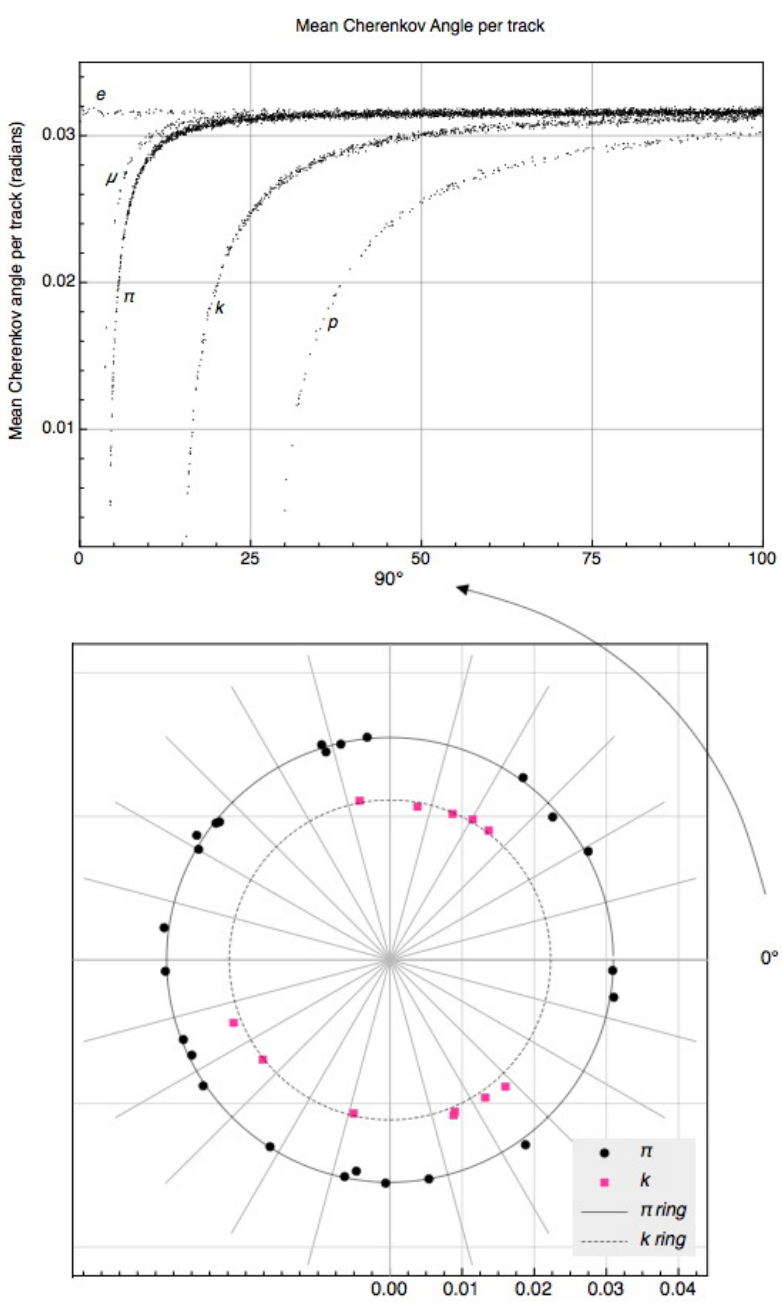

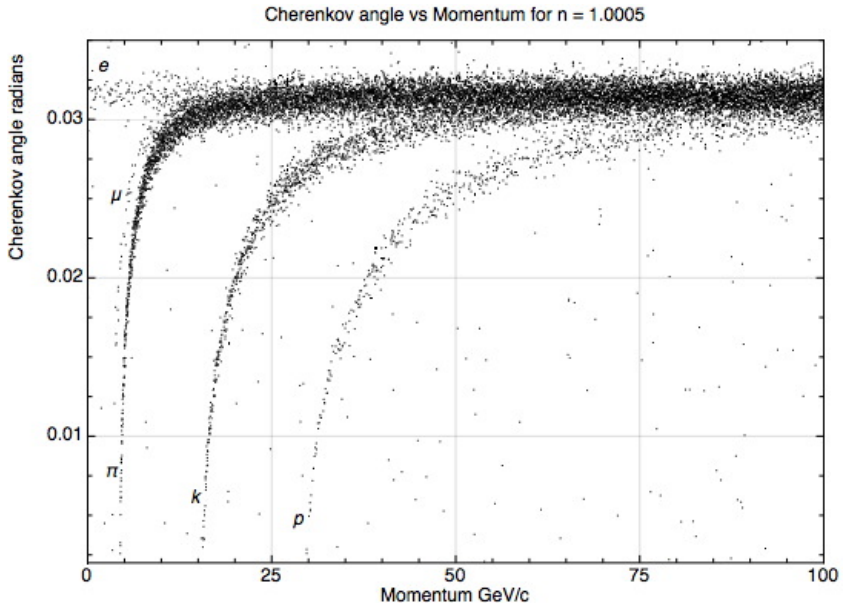

Cherenkov photons emitted by a 22 GeV/c pion or kaon

Examples of fixed-target experiments:

NA-62 at CERN

KOTO at J-Parc

The K→ πνν decays in the Standard Model

- FCNC loop processes: s→d coupling and highest CKM suppression

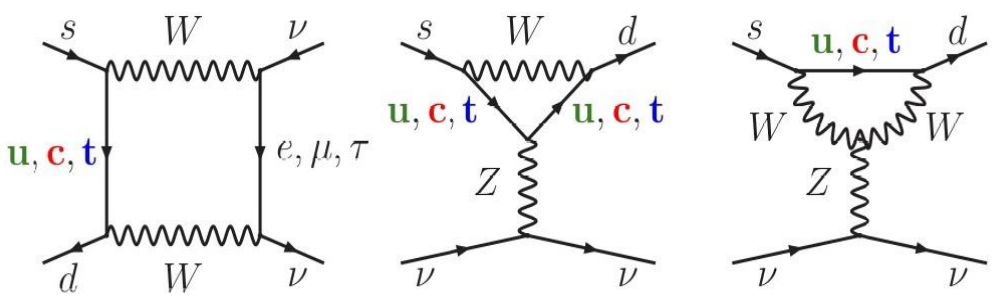

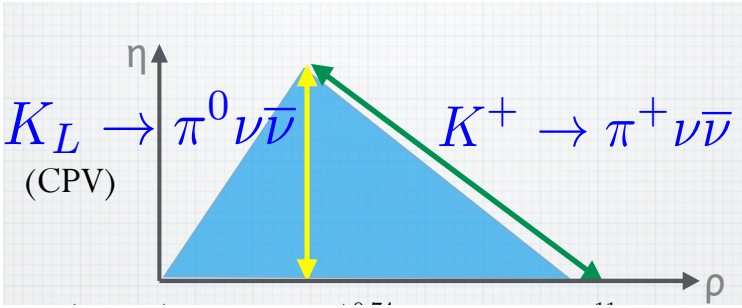

- Very clean theoretically: Short distance contribution. No hadronic uncertainties.
- SM predictions [Buras et al. JHEP 1511 (2015) 33]

$$\mathrm{BR}(K^+ \to \pi^+ \nu\bar{\nu}) = (8.39 \pm 0.30) \cdot 10^{-11} \left(\frac{|V_{cb}|}{0.0407}\right)^{2.8} \left(\frac{\gamma}{73.2°}\right)^{0.74} = (8.4 \pm 1.0) \cdot 10^{-11}$$

$$\mathrm{BR}(K_L \to \pi^0 \nu\bar{\nu}) = (3.36 \pm 0.05) \cdot 10^{-11} \left(\frac{|V_{ub}|}{0.00388}\right)^{2} \left(\frac{|V_{cb}|}{0.0407}\right)^{2} \left(\frac{\sin\gamma}{\sin 73.2}\right)^{2} = (3.4 \pm 0.6) \cdot 10^{-11}$$

- Experiments:

(BNL E787+E949)

$\mathrm{BR}(\mathrm{K}^+ \to \pi^+ \nu\bar{\nu}) = \left(17.3^{+11.5}_{-10.5}\right) \times 10^{-11}$ Phys. Rev. D 77, 052003 (2008), Phys. Rev. D 79, 092004 (2009)

$\mathrm{BR}(\mathrm{K_L} \to \pi^0 \nu\bar{\nu}) < 2.6 \times 10^{-8}$ (90% C. L.) Phys. Rev. D 81, 072004 (2010) (KEK E391a)

K→ πνν decays and New Physics

New physics affects BRs differently for K^+ and K_L channels

Measurements of both can discriminate among NP scenarios

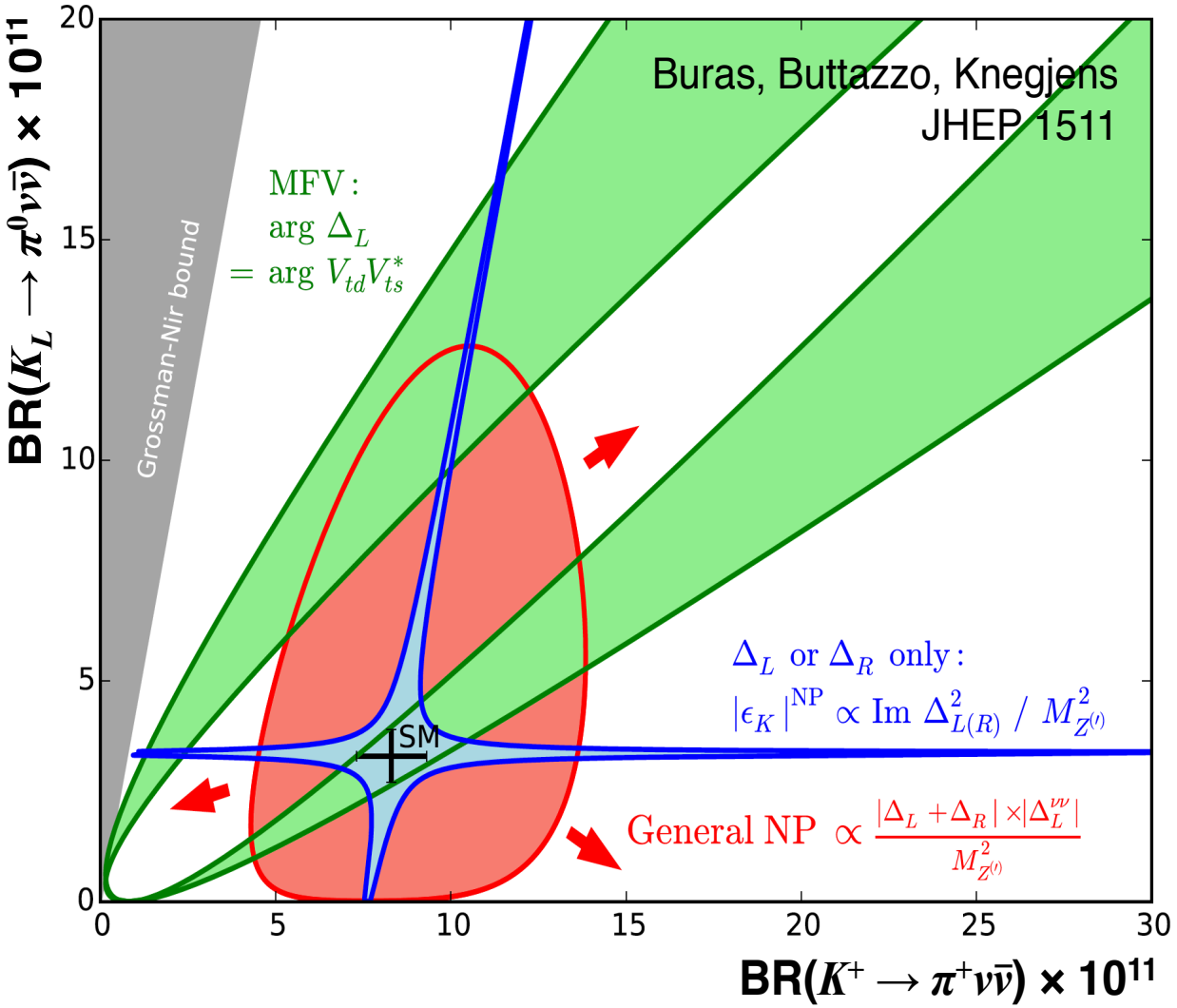

- Models with CKM-like flavor structure
  - Models with MFV
- Models with new flavor-violating interactions in which either LH or RH couplings dominate
  - Z/Z' models with pure LH/RH couplings
  - Littlest Higgs with T parity
- Models without above constraints
  - Randall-Sundrum

$K^+ \rightarrow \pi^+ \nu\nu$ decay at NA62 - CERN

NA62: guiding principles

- Kinematic rejection (m^2_{miss}):
  - Minimal amount of material budget:
    - X/X_0 kaon spectrometer (Gigatracker, Si pixel): 1.5% total
    - X/X_0 pion spectrometer (Straw Chambers in vacuum) < 2% total
- Precise timing for K-π matching:
  - Gigatracker time resolution: < 200 ps / station (beam test results on a prototype)
  - RICH time resolution: < 80 ps [NIM A 593 2008]
- High efficiency photon veto:
  - 10^{-8} π^0 veto inefficiency in $K^+ \to \pi^+\pi^0$ events
    - Offline analysis trick: $P_{\pi+} < 35$ GeV/c $\to E_{\pi0} > 40$ GeV
    - 10^{-5} LKr inefficiency for $E_\gamma > 10$ GeV
    - Hermeticity up to 50 mrad and down to 500 MeV photons (LAV detectors)
- Particle ID
  - MUV and RICH for μ–π separation → totally independent ID methods
  - LKr and RICH for π–e separation → totaly indepedent ID methods
  - Cerenkov threshold counter on beam to control the beam induced background

$K^+ \to \pi^+ \nu\nu$ decay at NA62 - CERN

- Taking physics data since 2015
- Will measure BR($K^+ \to \pi^+ \nu\bar{\nu}$) to 10% by end of 2018
  100 signal events, $S/B \sim 5$

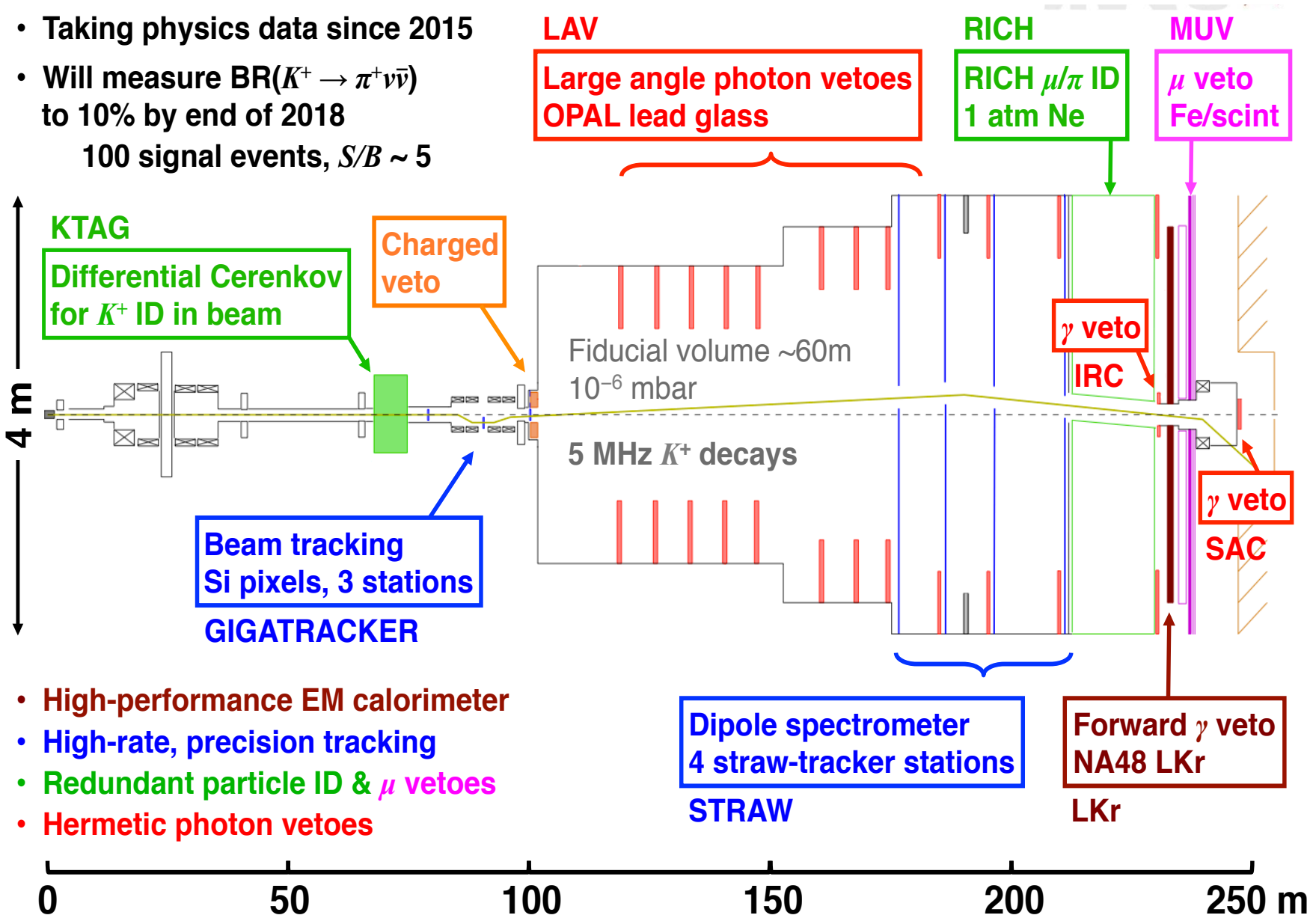

- High-performance EM calorimeter
- High-rate, precision tracking
- Redundant particle ID & μ vetoes
- Hermetic photon vetoes

NA62 data quality studies

1-track selection require K^+ ID in KTAG

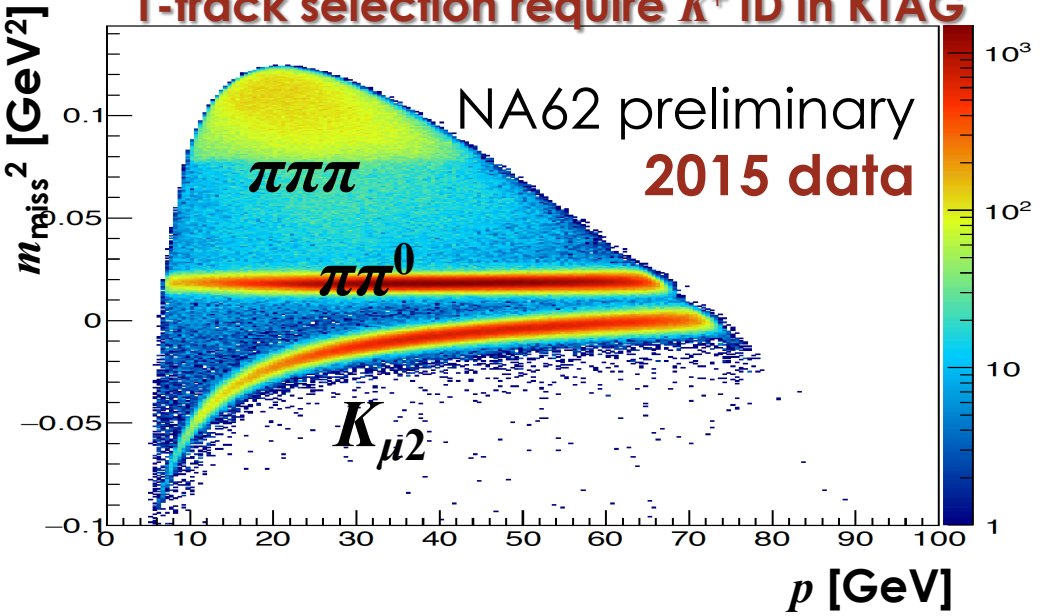

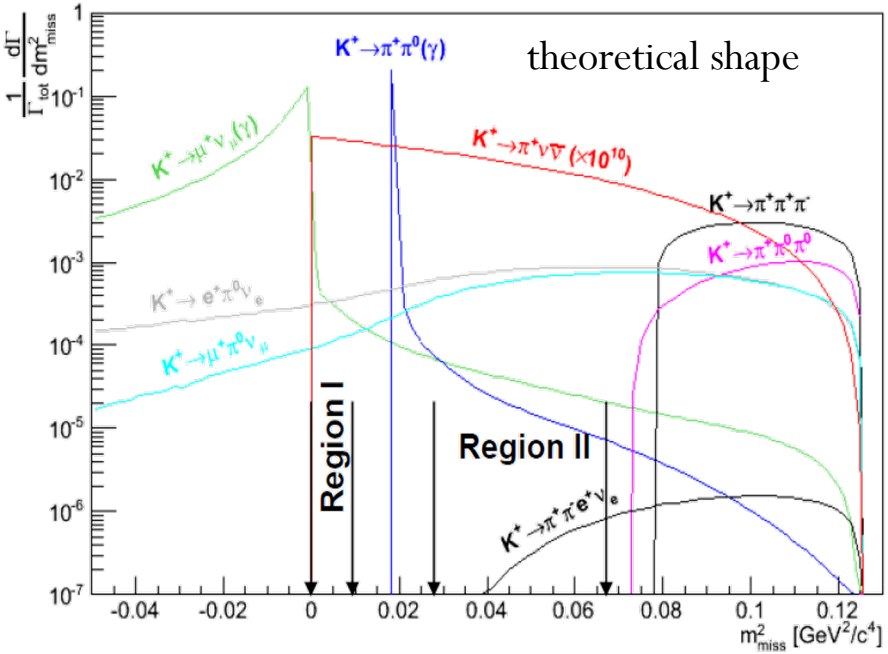

RICH ring radius vs track momentum

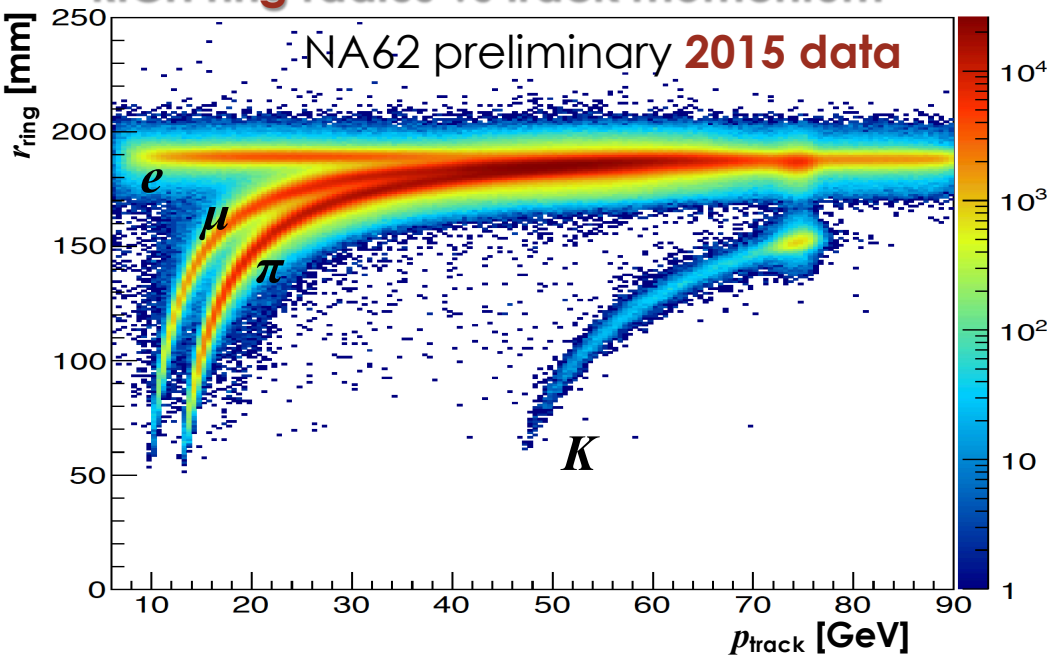

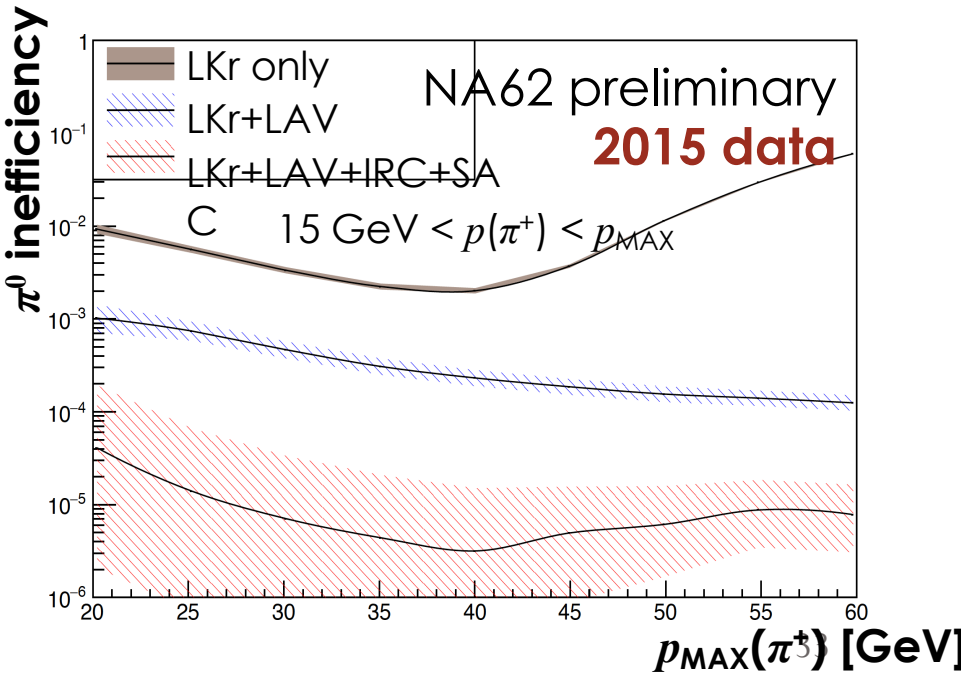

First NA62 result on πνν

- **See talk by Z. Kucerova, this conf.**
- 2% of total 2016-2018 exposure
- 0.27 SM signal evts expected, 0.15 backgorund
- First successful application of in-flight technique

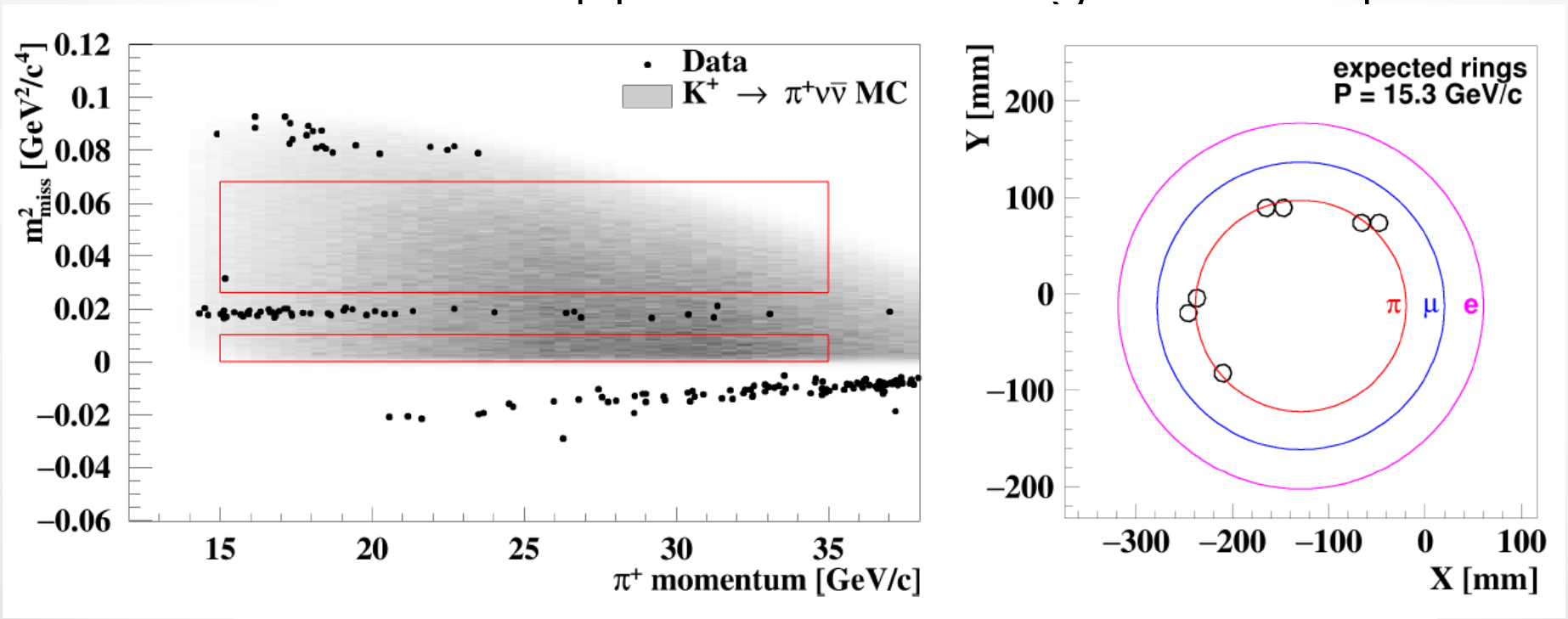

$$\mathrm{BR}(K^+ \to \pi^+ \nu\bar{\nu}) < 14 \times 10^{-10} \text{ at } 95\% \text{ CL.}$$

Status of $K_L \to \pi^0 \nu\nu$

- Experimental limit : 2.6×10^{-8} (KEK E391a)
- Indirect limit : 1.5×10^{-9} (Grossman-Nir)

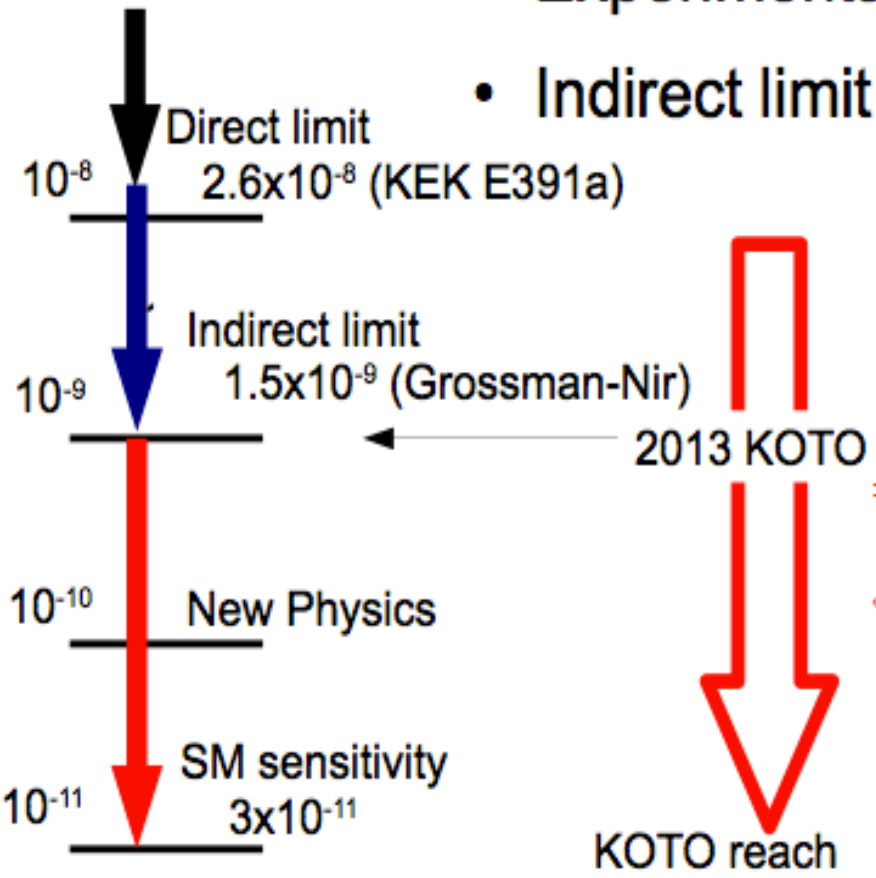

Br($K^+ \to \pi^+ \nu\nu$) and isospin rotation

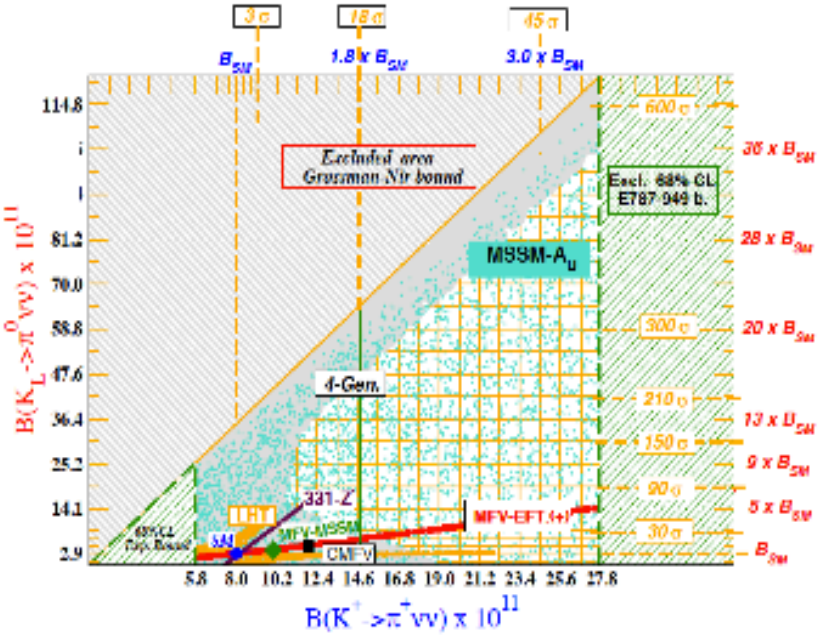

KOTO aim to improve the sensitivity by 3 order!
to search for CPV new physics. (~ 3 SM events)

J-PARC
Hadron Hall

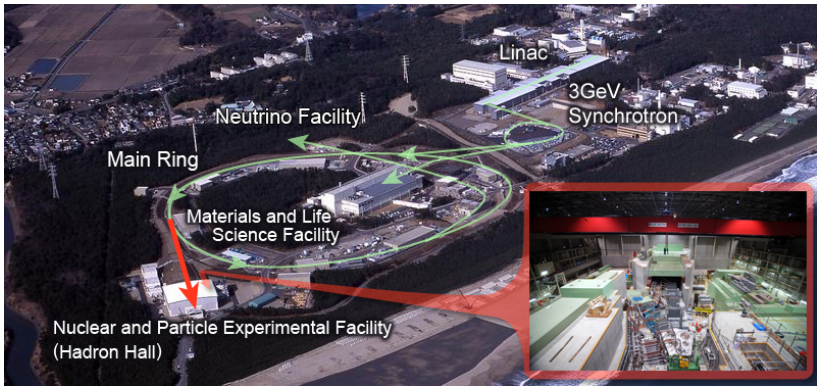

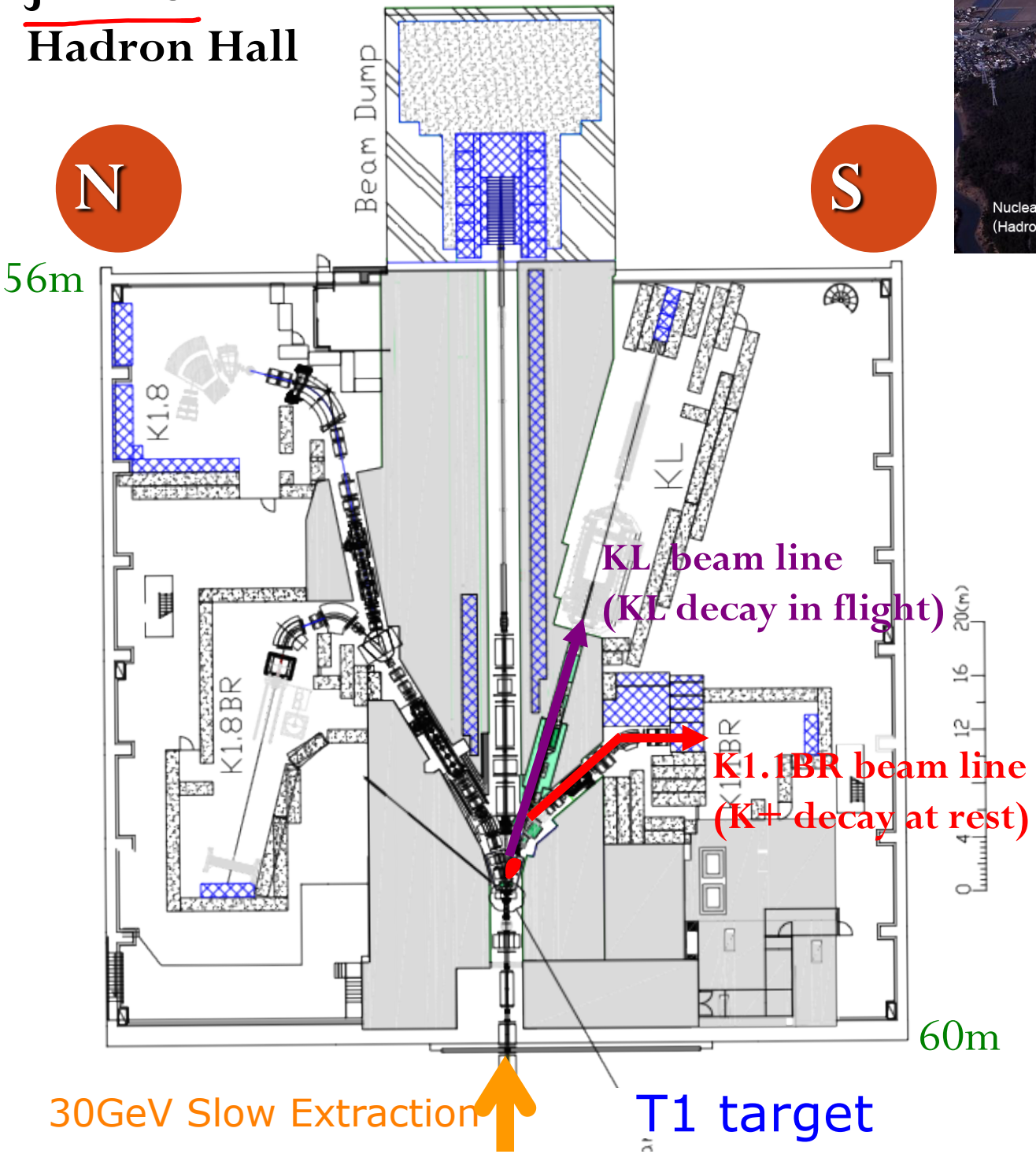

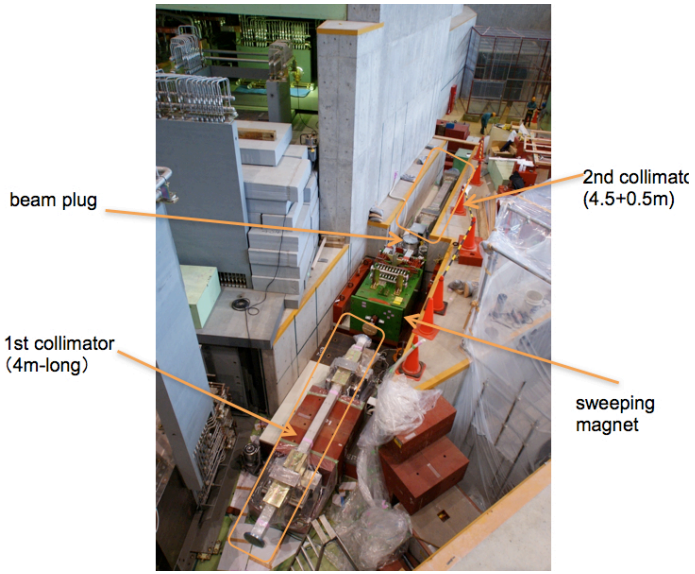

J-PARC
Hadron Hall

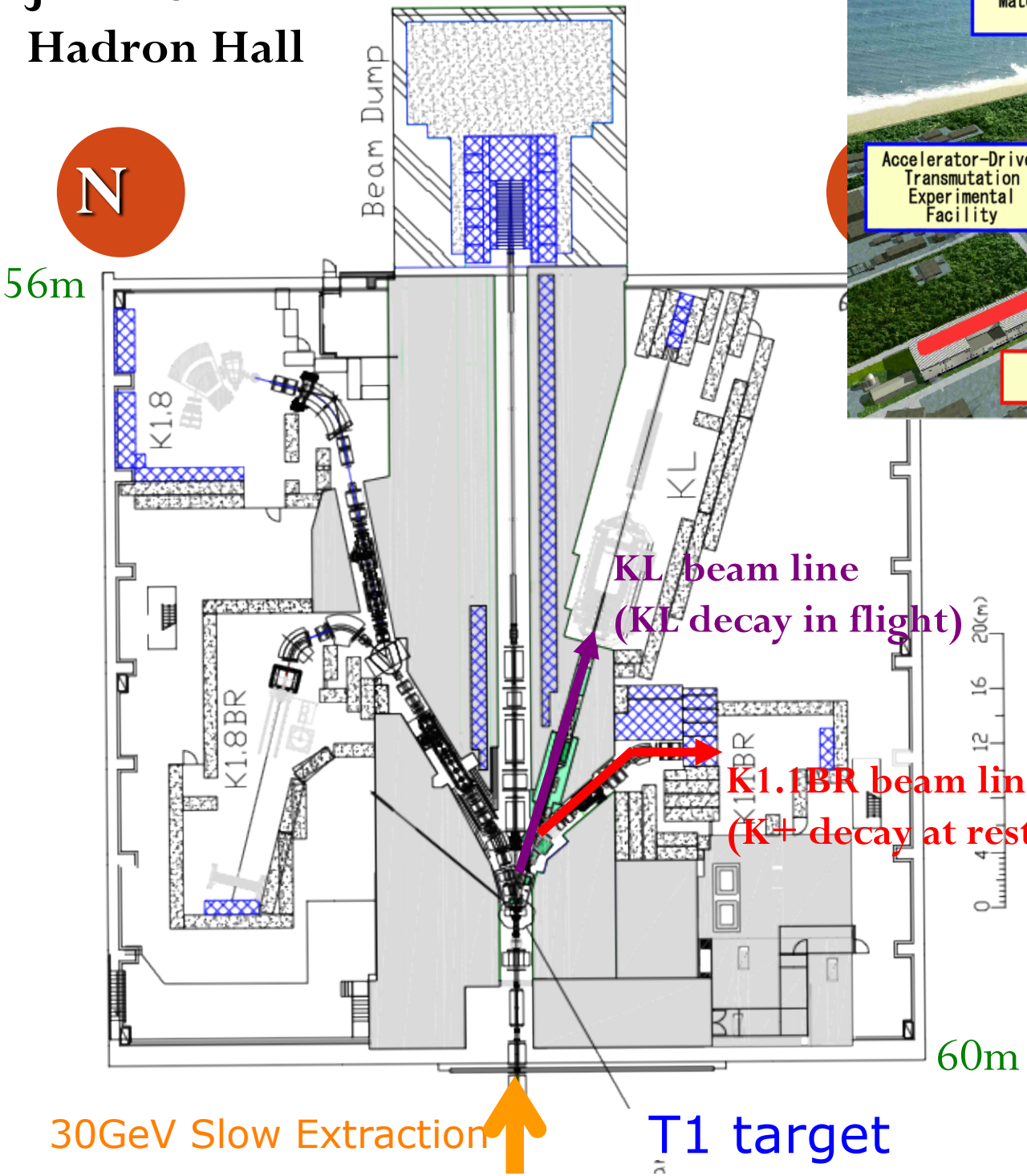

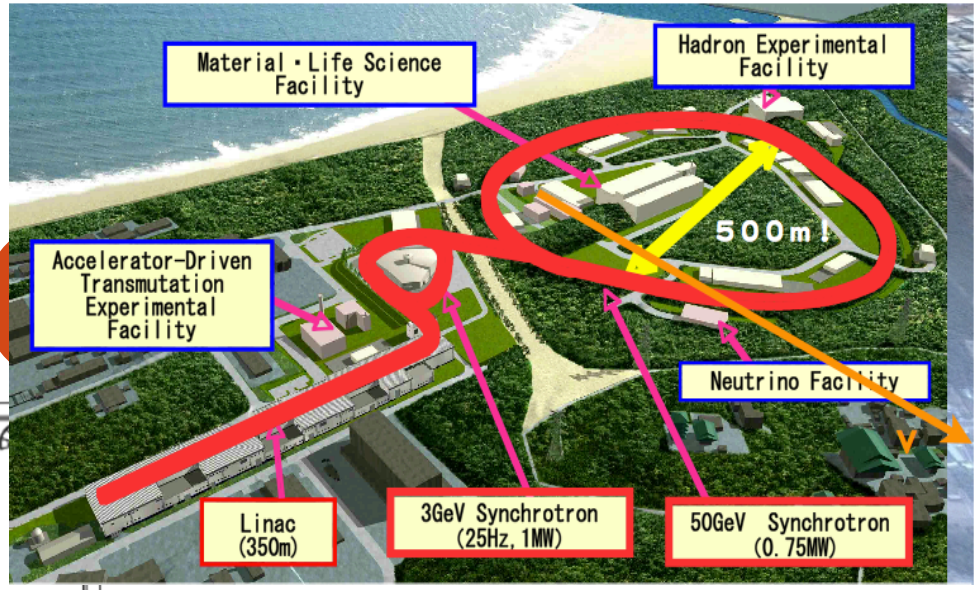

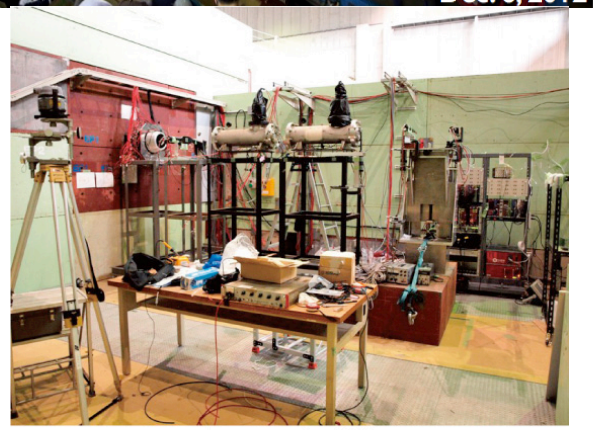

$K_L \rightarrow \pi^0 \nu\nu$ at KOTO - JPARC

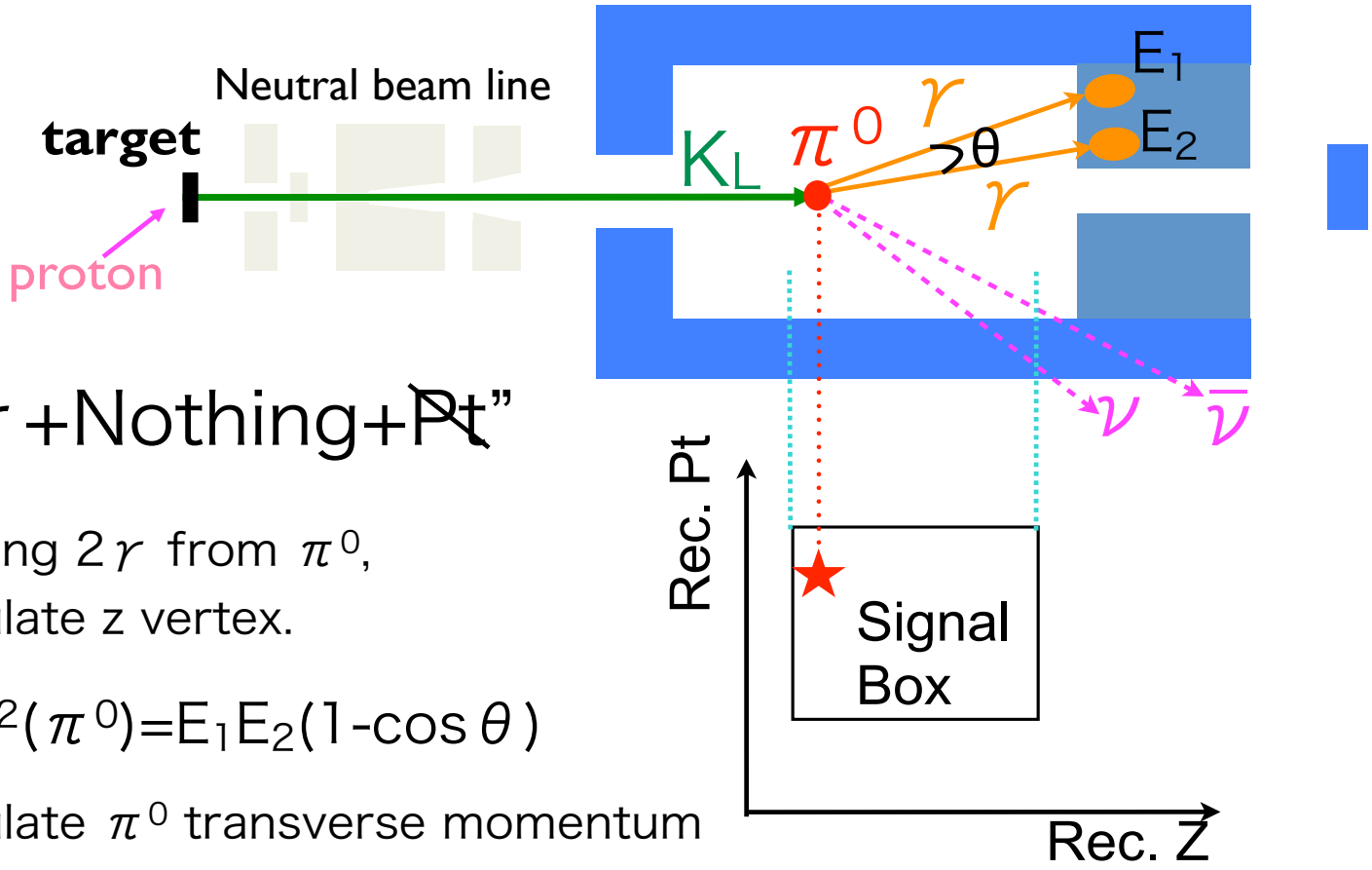

"2γ +Nothing+$\not{P}_t$"

Assuming 2γ from π^0,
Calculate z vertex.

$$M^2(\pi^0)=E_1E_2(1-\cos\theta)$$

Calculate π^0 transverse momentum

- Vertex reconstruction with pi0 mass and vtx on z-axis assumption
  - Fiducial region in z ↔ neutron background
  - π^0 Pt reconstruction → High Pt selection

CKM2012

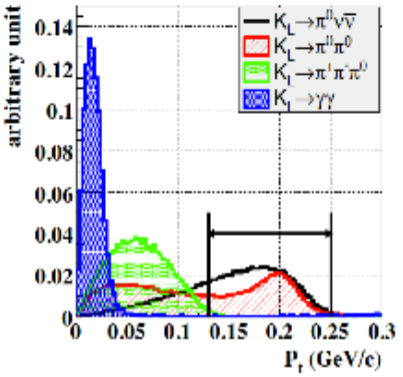

KOTO detector

CsI calorimeter + Hermetic veto system

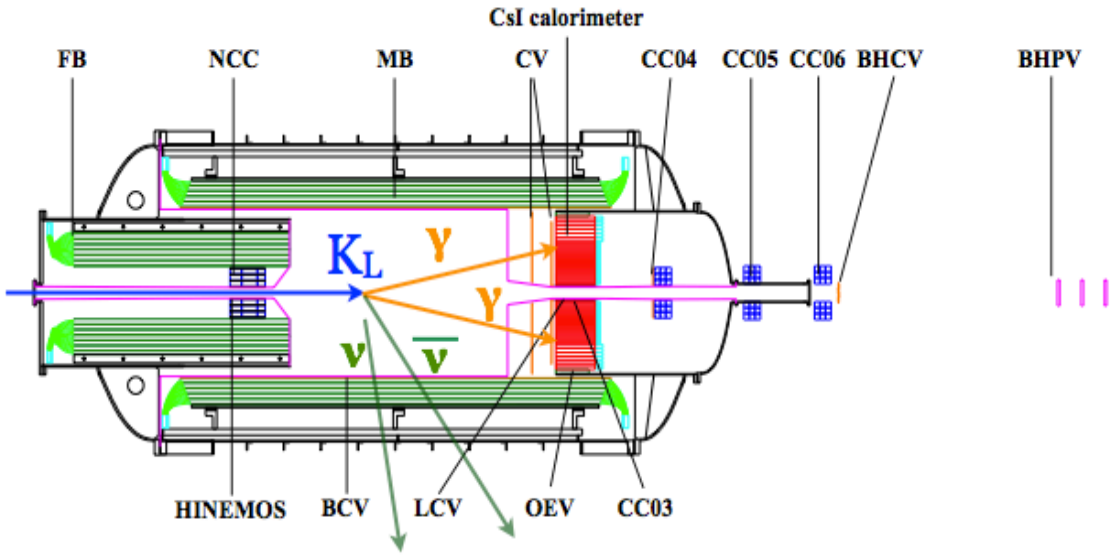

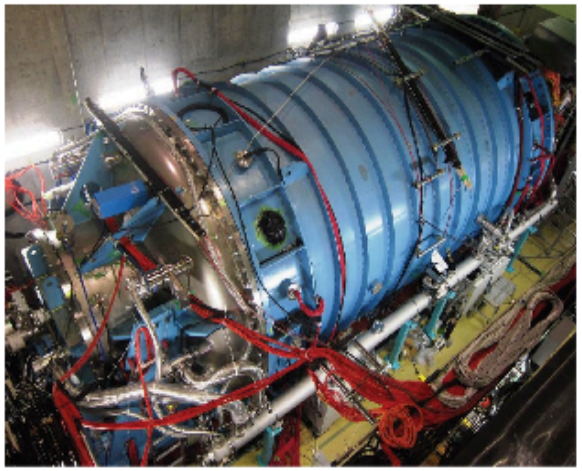

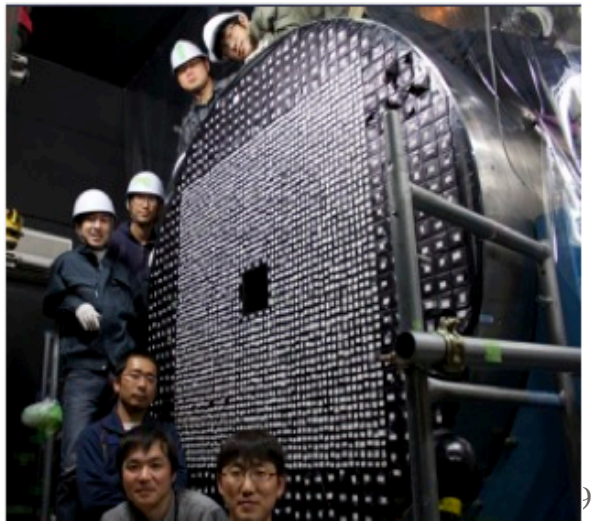

We installed all detectors by May 2013.

KOTO data taking

2013 first physics run (run49)
-100 h with 24 kW beam (10% of design intensity)
-single event sensitivity (ses) of 1.3 x 10^{-8}
(nearly the same as in E391a: 1.1 x 10^{-8})
BR($K_L \to \pi^0\nu\nu$) < 5.1 x 10^{-8} (90% C.L.)
submitted PTEP arXiv:1609.03637

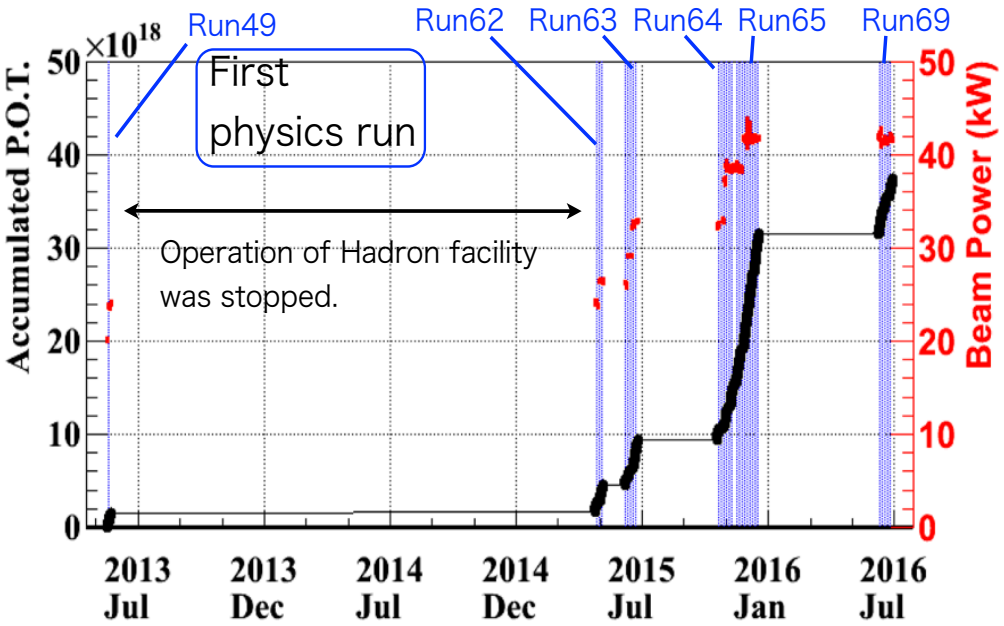

2014 Understanding the background (see next slide) and upgrade of downstream detector

2015 Physics run (aims to ses at GN bound)
-prelim. result on run62: ses of 5.9 x 10^{-9}
2015 upgrade to further suppress $K_L \to 2\pi^0$ bkg: additional barrel photon detector (Inner Barrel)

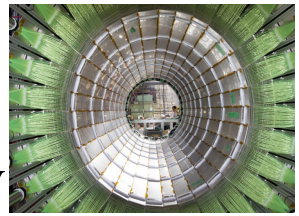

2018 add MPCCs on CSI calorimeter
2019 beam power 42 kW -> 100 KW

KOTO data taking

2013 first physics run (run49)
-100 h with 24 kW beam (10% of design intensity)
-single event sensitivity (ses) of 1.3 x 10^{-8}
(nearly the same as in E391a: 1.1 x 10^{-8})
BR(K_L □ $\pi^0\nu\nu$) < 5.1 x 10^{-8} (90% C.L.)
submitted PTEP arXiv:1609.03637

2014 Understanding the background (see next slide) and upgrade of downstream detector

2015 Physics run (aims to ses at GN bound)
-prelim. result on run62: ses of 5.9 x 10^{-9}
2015 upgrade to further suppress $K_L \rightarrow 2\pi^0$ bkg: additional barrel photon detector (Inner Barrel)

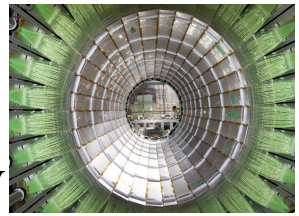

2018 add MPCCs on CSI calorimeter
2019 beam power 42 kW -> 100 KW

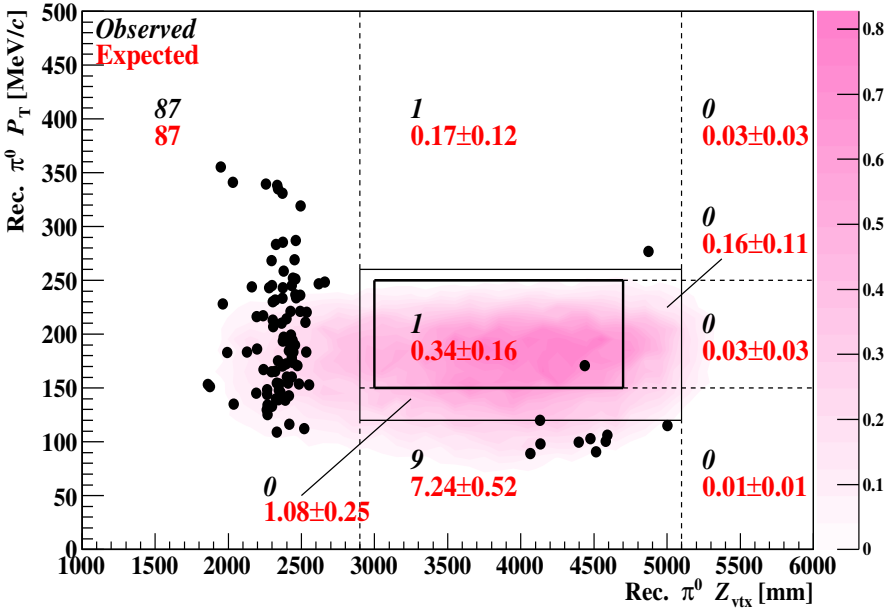

Lessons from first Physics run

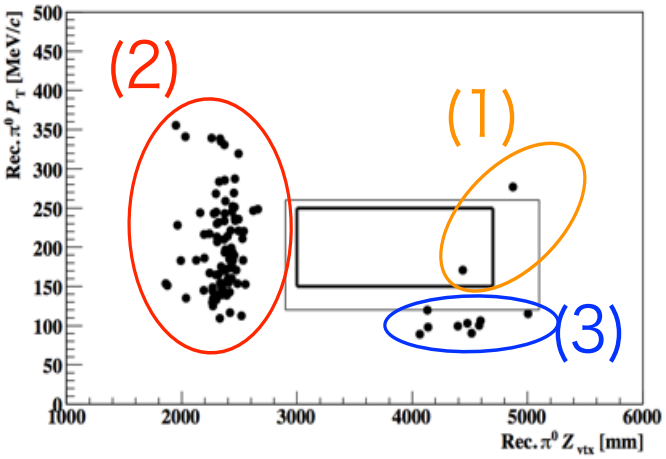

(1)Halo neutrons hitting the CsI Calorimeter

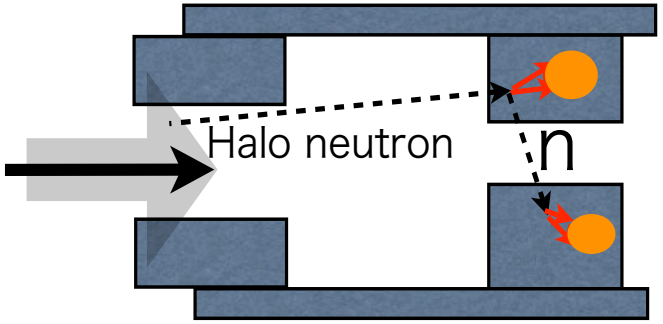

(2)Halo neutrons hitting the NCC

(3)$K_L \rightarrow \pi^+\pi^-\pi^0$ BG

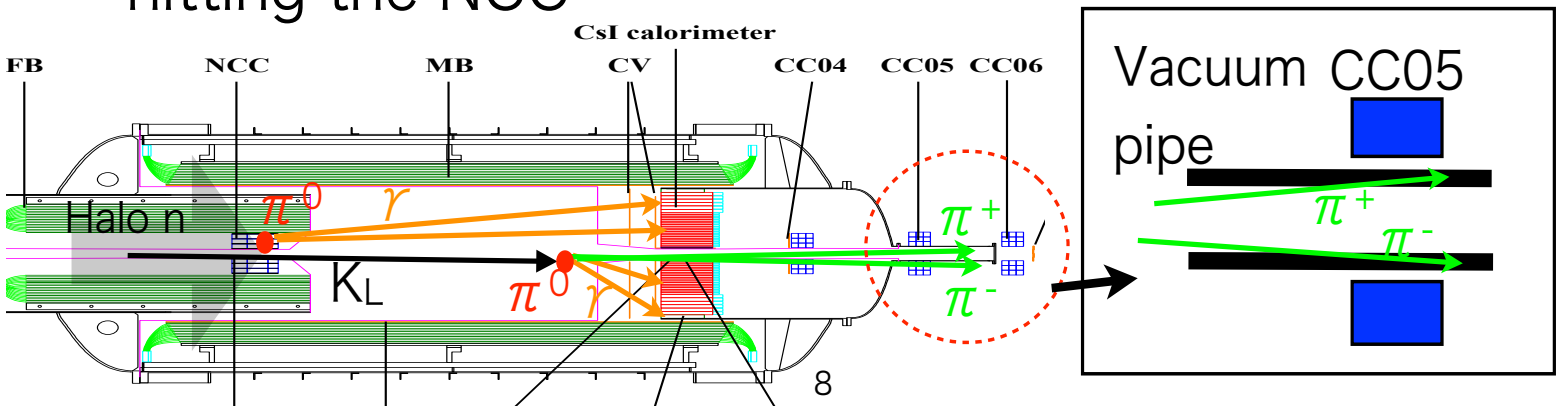

2013-2014 upgrades

Against KL->p+p-p0 : Replaced the vacuum pipe with thinner one; Installed new scintillator counters

Against neutron bkg: Beam Profile Monitor

Against KL-2p0: additional photon counters

For high intensity: In-beam Charged Veto (Wire chamber CF4+C5H12 gas)